Graphical design of gas-liquid reactors

D. W. VAN KREVELEN and P. J. HOFTYZER

Staatsmijnen in Limburg, Central Laboratory, Geleen, The Netherlands

Summary—The rate of a gas-liquid reaction is determined by the contact surface between the phases as well as by the coefficients of mass transfer in gas and liquid, the reaction rate constant, the diffusion coefficient and the concentrations of the two components. Dimensional analysis provides a means for determining number and character of the dimensionless quantities that govern the process. By means of the absorption mechanism according to the film concept, the functional relationship between these dimensionless quantities is determined and expressed in a graph.

A graphical method is developed for designing absorption apparatus in which also chemical reactions occur. The method enables one to determine the course of the driving force in the gas phase as a function of the composition of gas and liquid. By plotting the reciprocal value of the driving force versus the partial pressure in the gas phase and by integration the number of " transfer units " can be found.

The applicability of the derived relationship, is subjected to a critical study. The uncertainty of the actual active area in a packed column makes the design of this apparatus difficult. Non-uniformity of wetting in a packed column may have a very adverse influence on the operation of the apparatus and hence on the applicability of any method of design.

Résumé—La vitesse d'une réaction gaz-liquide est controlée par la surface de contact entre les phases, par les coefficients du transport de la matière dans le gaz et le liquide, par la constante de la vitesse de reaction, par le coefficient de diffusion, enfin par les concentrations des deux composants. L'analyse dimensionelle nous procure un moyen pour déterminer le nombre et le caractère des grandeurs sans dimensions qui dominent le processus. Utilisant comme modèle d'opération le mécanisme d'absorbtion au travers d'une couche de passage "film," on determine la relation fonctionnelle entre ces grandeurs sans dimensions que l'on inscrit sur un graphique.

Les auteurs développent une méthode graphique pour calculer les appareils d'absorbtion dans lesquels se produisent aussi des réactions chimiques. La méthode permet de déterminer la variation de la force motrice dans la phase gazeuse en fonction de la composition du gaz et du liquide. Représentant l'inverse de la force motrice en fonction de la pression partielle dans la phase gazeuse, on peut trouver par intégration le nombre des " unités de transport."

L'hypothèse servant de base à cette méthode, à savoir l'applicabilité de la relation derivée, est soumise à un examen critique. L'incertitude sur la valeur de la surface vraiment active dans un scrubber rend difficile le calcul de cet appareil. Il faut signaler que la non-uniformité du mouillage dans un scrubber peut exercer une influence très défavorable sur son fonctionnement et donc sur la validité de toute méthode de calcul de ce type d'appareil.

INTRODUCTION

In many chemical processes gas-liquid reactions play an important role. However, in chemical engineering these processes have received little attention. As a rule the subject is treated as a part of the unit operation " gas absorption," namely as an absorption combined with chemical reactions. For a survey of the literature on this subject, we refer to the monograph by SHERWOOD and PIGFORD [7].

The mechanism of the process of gas-liquid reactions can be described as follows : a component A in the gas phase is to react with a component B in the liquid. The component A

in the gas is first transported to the phase boundary. It is assumed that at the phase boundary proper the gas immeasurably rapidly establishes equilibrium with the liquid; at the interface component *A* dissolves physically. Then, the dissolved component *A* is transported from the phase boundary into the liquid whereas component *B* is transported from the bulk of the liquid towards the interface. During this transport *A* and *B* react with each other in a reaction zone running parallel to the interface. Finally, the reaction product is transported out of the reaction zone.*

The foregoing may be formulated with the help of Fig. 1 and 2. Fig. 1 shows the concentration profile in the gas and liquid phases for the case of a *purely physical absorption*, Fig. 2 holds for *absorption combined with chemical reaction*. In
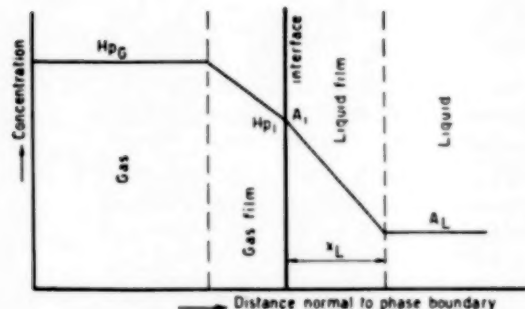

Fig. 1. Concentration profile for physical absorption

both figures the driving force in the gas phase is equal to $p_G - p_i$. The mass transfer coefficient in the gas phase, k_G, is defined by the equation :

$$\dot{n} = k_G (p_G - p_i)$$

The equilibrium at the interface is described by : $A_i = H p_i$. In the case of physical transport of *A* from the phase boundary without a chemical reaction (by a driving force $= A_i - A_L$, Fig. 1),

___

* If the reaction rate is immeasurably high, the above picture is modified in the sense that the reaction zone becomes infinitely thin and frequently substantially coincides with the phase boundary. For a complete description of the concentration profiles we refer to a previous paper [9].
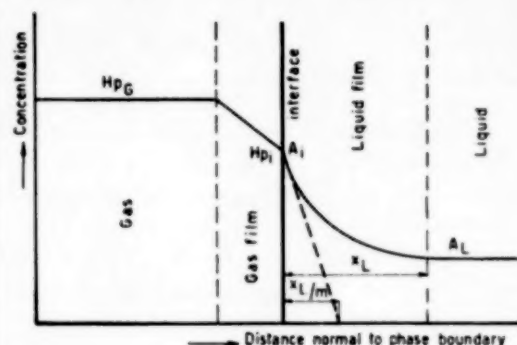

Fig. 2. Concentration profile for absorption with chemical reaction

we are only concerned with the coefficient of mass transfer in the liquid k_L :

$$\dot{n} = k_L (A_i - A_L)$$

The occurrence of a chemical reaction accelerates the removal of *A* from the interface. The degree of this acceleration may be expressed by the multiplication factor *m* so that :

$$\dot{n} = m k_L (A_i - A_L)$$

The importance of the factor *m* can be demonstrated by means of the film concept. In Fig. 1 the concentration profile through the liquid film having a thickness x_L, is represented by a straight line, so that $k_L = \dfrac{D}{x_L}$. In Fig. 2, the component *A* is eliminated by chemical reaction during the transport from the phase boundary. This explains why the concentration profile in this case is represented by a curved line. The dotted line gives the concentration profile if – at the same rate of absorption – component *A* should only be removed by diffusion. Then, the effective diffusion path is apparently *m* times smaller than the total film thickness x_L. From this it follows that :

$$\dot{n} = \frac{D}{x_L/m} (A_i - A_L) = m k_L (A_i - A_L)$$

Now, the point at issue is to express the factor *m*, which represents the acceleration of the absorption due to the chemical reaction, as a function of known quantities. To this end,

dimensional analysis will be used, which reduces considerably the number of variables.

Dimensionless Products and their Functional Relationship

A general method for the derivation of the dimensionless products occurring under given conditions was developed by Langhaar [4].

The variables considered are $\dot{n}$, A, B, D, k_L, k, because all of them are either measurable or given. It might be possible to part the problem more generally and to consider a larger number of variables; the above selection consequently implies some simplifying assumptions. The quantity " time " for example, has been left out of account so that the treatment is limited to steady state processes.

Dimensional analysis yields the following three dimensionless products : A/B, $\dot{n}/k_L A$, kDB/k_L^2.

Dimensional analysis does not give any information about the functional relationship between the dimensionless products. The latter can be found starting from a given picture for the mechanism of mass transfer from the interface. The best known and most commonly used picture is that of the film concept. Its feature consists in the assumption of a laminarly flowing liquid film at the phase boundary.

A derivation of the relationship between the three dimensionless products based on the film concept, has been given by the authors in a previous paper [10]. The result of the calculations can be summarized in the graph shown in Fig. 3. In this graph $m (= \dot{n}/k_L A_i)$ has been plotted versus $(kDB_L)^{\frac{1}{2}}/k_L$ in a bundle of lines each of which represents a given value of B_L/A_i. When 1 mol of A reacts with z moles of B, the quantity B_L/zA_i must be used in the graph.

A closer view of Fig. 3 will show that under some special conditions the relationship between the dimensionless products becomes very simple.

1. If k (so $kDB_L)^{\frac{1}{2}}/k_L$ is very small, m equals unity. In this case one is concerned with physical absorption.

2. If k is very great, $m \approx B_L/zA_i$, or $\dot{n} = k_L B_L/z$. Here the rate of the process is determined by the transport of component B towards the phase boundary.

3. At moderately high values of k it is often found that $m = (kDB_L)^{\frac{1}{2}}/k_L$, which case is represented by the straight line running through the graph at an inclination of 45°. This means that $\dot{n} = A_i (kDB_L)^{\frac{1}{2}}$, i.e. the rate of the process is exclusively determined by the rate of the chemical reaction.

Besides the film concept, the picture which Danckwerts [1] has developed for the mechanism of mass transfer in the liquid, may be used as a model. According to this picture it is assumed that a liquid element at the interface will absorb component A for a certain length of time, whereafter it is exchanged against a fresh liquid element. For steady state processes, it is assumed that the residence times of the elements of liquid at the phase boundary are distributed statistically between the values zero and infinite. A general solution of the relationship between the three dimensionless products according to this concept has not yet been found. However, also here the three aforementioned special cases may be distinguished, the solution of which is identical to that according to the film concept.

In principle, the foregoing makes it possible to calculate the rate of the process per unit surface,
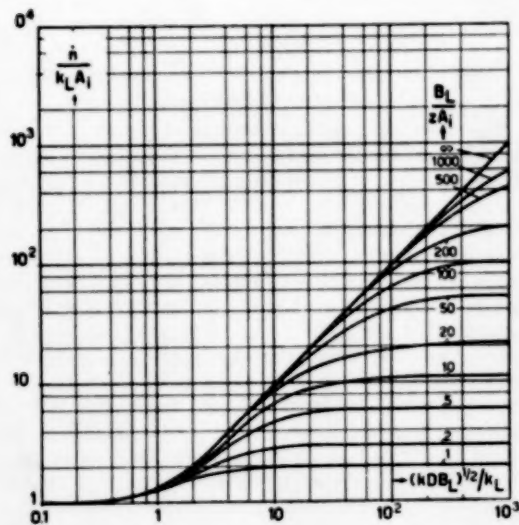

Fig. 3. Relationship between dimensionless products, $\dfrac{\dot{n}}{k_L A_i}$, $\dfrac{(kDB_L)^{\frac{1}{2}}}{k_L}$, $\dfrac{B_L}{zA_i}$

$\dot{n}$, if the quantities A_i, B_L, D, k_L and k are given. For the calculation of A_i we need also the quantity k_G.

The coefficients of mass transfer must generally be derived from experimental data. In this case always the products $k_G a$ and $k_L a$ are found, being identical with the coefficients expressed per unit volume of the apparatus. Only if a, the effective area per unit surface, is known can k_G and k_L be calculated therefrom. Formulae for the calculation of k_G and k_L in a packed column are available [12]. The relationship for k_G was derived by the authors on the analogy of tests on the rate of evaporation at the surface of solid substances and reads :

$$\frac{k_G RT}{a_p D} = 0.22 \left(\frac{u_G \rho}{a_p \mu}\right)^{0.8} \left(\frac{\mu}{\rho D}\right)^{0.4}$$

The relationship for k_L was derived from the tests by SHERWOOD and HOLLOWAY [6] assuming that the packing material was completely wetted. It reads :

$$\frac{k_L}{a_p D} = 5 \left(\frac{u_L \rho}{a_p \mu}\right)^{4} \left(\frac{\mu}{\rho D}\right)^{0.4}$$

The chemical reaction rate constant k is available for a few systems only, e.g. for the absorption of carbon dioxide in lye and ammonia solutions [11]. Furthermore, it is known that for a number of systems the reaction rate is immeasurably high : reactions of acetic acid, hydrogen sulphide, hydrogen cyanide and sulphur dioxide with lye, and of ammonia with a strong acid.

For an arbitrary unknown system either of the two following methods may be used ; measuring the reaction rate e.g. according to SAAL [5], or performing a model test in an absorption apparatus with a known contact surface e.g. a wetted-wall tower.

APPLICABILITY OF THE METHOD OF CALCULATION

Before treating the actual design of an apparatus for the performance of gas-liquid reactions, it is desirable to prove the validity of the above given functional relationship between the dimensionless products. There are many data available in literature about the rate of processes with combined absorption and chemical reaction, but most data deal with apparatus in which the actual contact area is unknown.

In the following two examples the method was applied to apparatus with known contact area, viz. absorption in a stirred batch apparatus and in a wetted-wall column.

It appears that the absorption rate for gas-liquid reactions in these apparatus can be predicted with reasonable accuracy, if the quantities A_i, B_L, D, k_L and k are given.

It is assumed here that the method may be applied to any type of absorption equipment. This assumption will need further approvement in future. The derivation of the functional relationship expressed in Fig. 3 with the aid of the film-concept might suggest that the application is limited to those cases where a viscous layer is actually present at the phase boundary. The identity of the solutions obtained with the concept of Danckwerts in some special cases, however, is an indication that the applicability of the solution might reach beyond this limitation.

Example 1

Batch Absorption of Carbon Dioxide in Potassium Hydroxide Solutions

Experiments on batch absorption of carbon dioxide in potassium hydroxide solutions have been carried out by HITCHCOCK [3]. In the same apparatus, under the same conditions of stirring, etc. the absorption of carbon dioxide in water supplied the value of $k_L = 9 \times 10^{-6}$ m/sec. From a study of the available data on batch absorption it was concluded that k_L is not changed very much by varying the viscosity of the solution. Therefore it is assumed that the same value of k_L may be used for interpreting the absorption in potassium hydroxide solutions.

As was shown on the foregoing pages, the rate of absorption with chemical reaction can be found with the aid of Fig. 3, which gives the functional relationship between the dimensionless products : A_i/B_L, $\dot{n}/k_L A_i$ and kDB_L/k_L^2. In these products A_i is the saturation concentration of carbon dioxide at the phase boundary, that can be calculated according to [13].

B_L is the concentration of potassium hydroxide. k is the reaction rate constant, which has the value of 1.05×10^4 m³/(sec.) (kgmol).

For three experiments with different values of B_L, the calculation of N_A is given below :

No.	B_L	$\frac{A_i}{10^{-2}}$	$\frac{D}{10^{-9}}$	$\frac{B_L}{A_i}$	$\frac{(kDB_L)^{\frac{1}{2}}}{k_L}$	$\frac{\dot{n}}{k_L A_i}$	$\frac{\dot{n}}{10^{-6}}$ calc.	$\frac{n}{10^{-6}}$ exp.
33	0·301	2·75	2·1	11	290	12	3·0	2·6
53	5·06	1·1	1·35	460	940	400	40	35
56	7·17	0·7	1·0	1020	960	600	38	39

The agreement between calculated and experimental values of $\dot{n}$ is very good. The table shows that for low values of B_L the transport of hydroxide ions to the phase boundary is 26 times slower than the chemical reaction and so determines the absorption rate. For high values of B_L, however, the reaction rate becomes slower than the transport of hydroxide ions.

Example II

Absorption of Carbon Dioxide by Ammoniacal Solutions in a Wetted-Wall Column

Some experiments on absorption of carbon dioxide by ammoniacal solutions in a wetted-wall column have been published by one of the authors in collaboration with C. J. van Hooren [11]. In that article a complete description of the experiments is given, so that this example will be restricted to some data that are illustrative for the applicability of Fig. 3. The following table compares calculated and experimental values of $\dot{n}$, for varying values of the initial ammonia concentration B_{Lo} and liquid rate per wetted perimeter Γ.

No.	$\frac{\Gamma}{10^{-2}}$	B_{Lo}	$\frac{B_L}{zA_i}$	$\frac{(kDB_L)^{\frac{1}{2}}}{k_L}$	$\frac{\dot{n}}{k_L A_i}$	$\frac{\dot{n}}{10^{-6}}$ calc.	$\frac{\dot{n}}{10^{-6}}$ exp.
4	1·09	0·31	3·2	8·0	3·5	6·8	6·1
12	1·59	1·32	16	16	10·5	21	23
19	6·66	3·11	51	18·5	15·5	42	36

The table shows that for low values of B_{Lo} and Γ, the absorption rate is determined by the rate at which ammonia can be supplied to the phase boundary. At higher values of B_{Lo} and Γ, however, chemical reaction determines the absorption rate.

GRAPHICAL METHOD IN DESIGN

The relationships given in the foregoing are valid at given concentrations of the components A and B in the gas and liquid phases. In practice, however, all concentrations vary from point to point through the apparatus. The only fixed concentrations are those of the in- and outgoing liquid and gas which are related through a material balance.

The course of the concentrations through the apparatus can be plotted in a graph.

Physical absorption

In its application to physical absorption this method is wellknown ; it is shown in Fig. 4. The vertical axis gives the partial pressure p of the gas component to be absorbed ; the horizontal
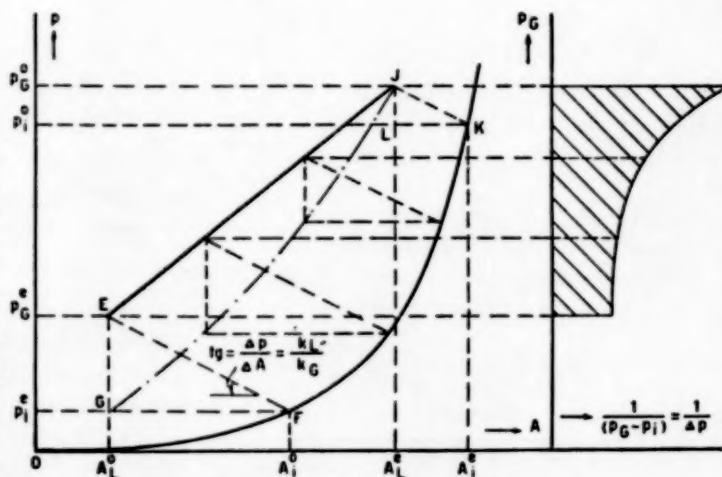

Fig. 4. Graphical design for physical absorption

axis shows the concentration of said component in the liquid A. The relation between p_G and A_L for every point of a counter-current apparatus is given by the operating line EJ, the equation of which reads :

$$\frac{dp}{dA} = \frac{u_L RT}{u_G}$$

The operating line passes through the points p^o_G, A^e_L and p^e_G, A^o_L ; it is straight if the volume of the passing gas mixture does not vary considerably during absorption.

The vapour tension of the solution as a function

149

of the concentration is given by the equilibrium line *OFK*.

Now, the construction is based on the equation for physical absorption :

$$\dot{n} = k_G (p_G - p_i) = k_L (A_i - A_L)$$

From various points on the operating line auxiliary lines are drawn to the equilibrium line at an inclination $= k_L/k_G$. The auxiliary line from E reaches the equilibrium line at F. The point F gives the conditions at the phase boundary where a gas of a pressure p^r_i is in equilibrium with a liquid having a concentration A^o_i. The driving force in the gas phase is $p^r_G - p^r_i = EG$; the driving force in the liquid is $A^o_i - A^o_L = GF$. So, at the given inclination of EF we find :

$$k_G (p^r_G - p^r_i) = k_L (A^o_i - A^o_L)$$

The same construction can be performed for other points of the operating line, e.g. in the triangle *JKL*.

Now that the driving force in the gas phase throughout the apparatus is known one may write for a layer of the apparatus with thickness dh :

$$\dot{n} = k_G (p_G - p_i) = \frac{u_G}{RTa} \frac{dp_G}{dh},$$

from which it follows that :

Number of transfer units =

$$N_G = \int_{p^o_G}^{p^r_G} \frac{dp_G}{p_G - p_i} = \frac{k_G RTa}{u_G} h = \frac{h}{H_{tG}}$$

If the height of a transfer unit for the apparatus used is known, the height of the apparatus itself can be calculated.[*]

[*] If the driving force in the gas phase becomes small as compared with that in the liquid, it is advantageous to base the calculation on the latter, for which case the following analogous equation holds :

$$\text{Number of transfer units} = N_L = \int_{A^o_L}^{A^o_L} \frac{dA_L}{A_i - A_L} = \frac{k_L a}{u_L} h = \frac{h}{H_{tL}}$$

The height of the column may also be calculated from the third term of the formula if the transfer coefficient in the gas phase k_G and the active area per unit volume a are given.

The right-hand half of Fig. 4 shows the graph

$$\frac{1}{(p_G - p_i)} = f(p_G)$$

by means of which the integration can be performed.
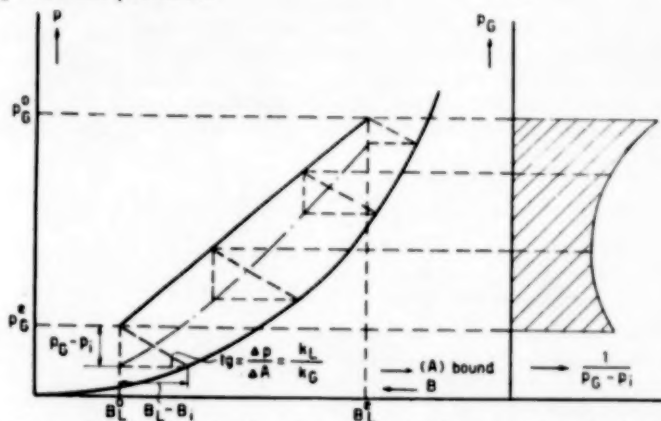

Fig. 5. Graphical design for absorption with fast reversible chemical reaction

Very fast chemical reaction

For absorption combined with a very fast reaction, in which case the rate of absorption is determined by the rate of transport of the second reacting component from the bulk of the liquid to the phase boundary, a graphical method of design may be used which is analogous to that for physical absorption. In Fig. 5 the partial pressure in the gas phase is plotted again along the vertical axis, the concentration of the chemically bound component A in the liquid being plotted along the horizontal axis. The concentration of the second reacting component B_L in the liquid may be plotted in the opposite direction along the same axis, in which case the operating line will give the relation between p_G and B_L.

Also here an equilibrium line has been drawn, giving the vapour tension of solutions as a function of the concentration of the chemically bound component A.

The construction is the same as the one used for chemical absorption ; from various points of the operating line auxiliary lines are drawn to the equilibrium line at an inclination $= k_L/k_G$.
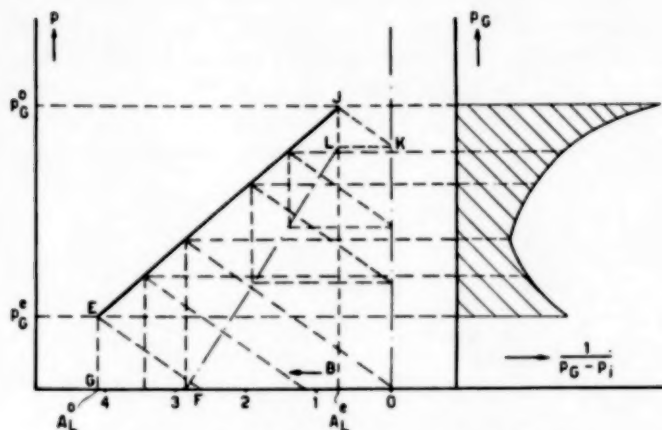

Fig. 6.   Graphical design for absorption with fast irreversible chemical reaction

The perpendicular of the resultant triangles indicates the driving force in the gas phase $p_G - p_i$; the base represents the driving force in the liquid $B_L - B_i$. Just like in Fig. 4 the number of transfer units N_G can be determined graphically.

In the foregoing it was assumed that in the reaction 1 mol of A corresponds with 1 mol of B. If in general 1 mol of A reacts with z moles of B, the auxiliary lines must be drawn at an inclination $= k_L/zk_G$.

A special case may present itself if the vapour tension of component A over the liquid is nil or very low. This situation is outlined in Fig. 6 which is of the same construction as Fig. 5. The scale used for B here has been graduated in arbitrary units. Because of the absence of an equilibrium line, the auxiliary line from point E of the operating line is drawn at an inclination $= k_L/k_G$ up to the abscissa and intersects the latter at F. FG represents the driving force in the liquid, $EG = p^e_G$ being the driving force in the gas.

For points in the operating line downwards from J however, the auxiliary line cannot be produced as far as the abscissa because the concentration of B at the phase boundary cannot fall below zero. At the point K on the auxiliary line drawn from J, $B = 0$, and JL represents the driving force in the gas at this point.[*]

The graph for $1/(p_G - p_i)$ as a function of p_G now yields a broken line.

Moderately rapid chemical reaction (reaction rate comparable with rate of mass transfer)

The case that an irreversible chemical reaction determines the rate of the process is represented in Fig. 7, where the operating line is drawn again in the customary manner. For any given point E of the operating line the rate of absorption $\dot{n}$ can now be found in the following manner. A certain value for the partial pressure in the gas at the phase boundary (p_i) is assumed. Then the transport velocity in the gas phase $= (p_G - p_i)k_G$. This must be equal to the value for $\dot{n}$ which can be found with the help of Fig. 3. The value for
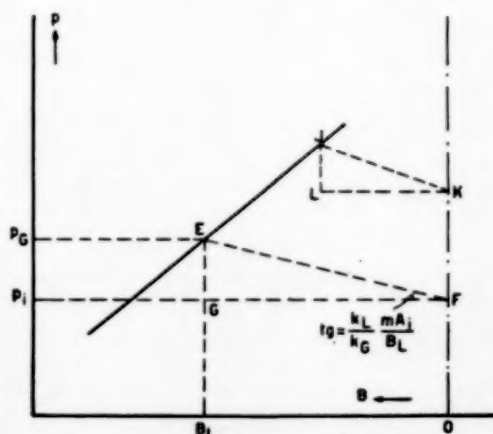

Fig. 7.   Graphical design for absorption with moderately rapid reaction

---

[*] Here it is assumed that the concentration of physically dissolved A at the phase boundary $A_i = Hp_i$ can be neglected with respect to B_L.

B_L to be used can be read from Fig. 7, while $A_i = Hp_i$.[*] If the value found for $\dot{n}$ does *not* correspond with the transport velocity in the gas phase, another value should be taken for p_i; in this way the correct value for the driving force in the gas phase can be found by trial and error. In the same way as was done in the previous cases the number of transfer units N_G can be determined graphically.

gas being equal to $p_G - p_i$, FG indicates the concentration in the liquid B_L. Now, however, the inclination of the line EF is $(p_G - p_i)/B_L$ $= \dot{n}/k_G B_L = \dfrac{k_L}{k_G} \cdot \dfrac{m A_i}{B_L}$. This quotient is always smaller than k_L/k_G; the deviation increases as m differs more from B_L/A_i. The same procedure has been performed for point J of the working line, giving triangle JKL, of which JL represents
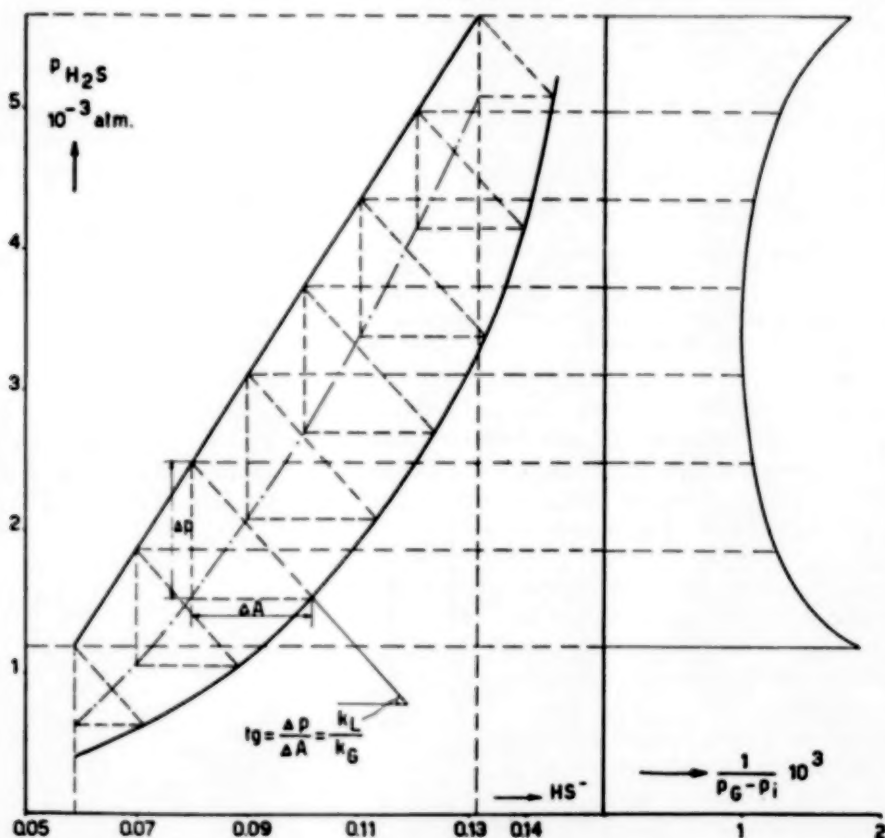
FIG. 8

Fig. 8

For comparison with the other figures the triangle EFG has also been drawn in Fig. 7. In this figure EG represents the driving force in the

the driving force in the gas phase and KL equals the concentration of component B. In this case the hypotenuse EF is no longer parallel to JK.

[*] For the Henry coefficient H the value for the electrolyte solution at the phase boundary must be used instead of the value for pure water. For method of calculation, see [13].

Examples

(a) *The design of a column for the absorption of hydrogen sulphide in sodium carbonate-bicarbonate solutions. Immeasurably rapid reaction; mass transfer is the determining factor.*

Data given :

Operating pressure 1 at. ; temperature 58°C. Quantity of gas 30,000 cu.m./hr containing 0·565 per cent by volume of H_2S ($p_g = 5·65 \times 10^{-3}$ at.); final content desired = 0·12 per cent. Amount of wash liquor 80 cu.m./hr. The alkalinity corresponds with 0·35 moles of Na_2CO_3 per litre. H_2S-content of the fresh liquid = 0·06 moles/1.

In Fig. 8 the operating line and the equilibrium line have been drawn for the above conditions. For the packing material used (wooden grids) and for the gas and liquid velocities applied ($u_G = 0·97$ m/sec and $u_L = 2·4·10^{-3}$ m/sec resp.) the quotient $k_L/k_G = 0·047$.

(b) Determination of the height of a column for the absorption of carbon dioxide in sodium hydroxide. Moderately rapid reaction which determines the rate of the process

Conditions given :

Pressure = 1 at., temperature = 21°C.

Diameter of the column = 6 inch, packing material ½ in. Raschig rings.

Superficial gas velocity = 0·216 m./sec. ; initial CO_2-content = 4·2 per cent-by volume ($p = 0·042$ at.); final content desired : 1·4 per cent (0·014 at.).

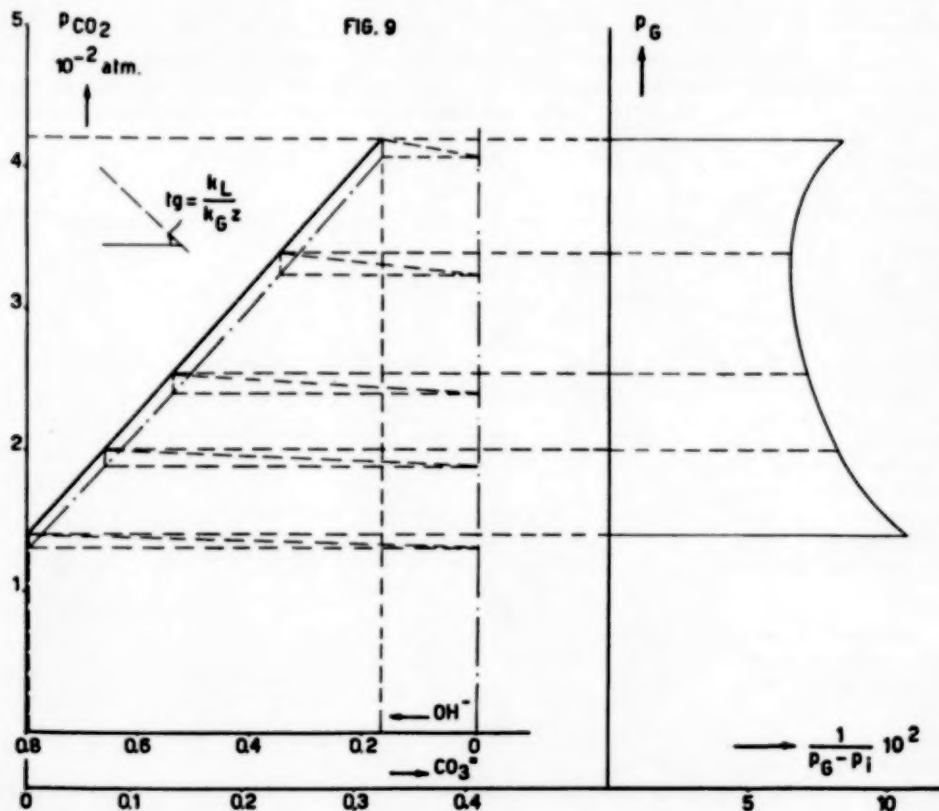Superficial liquid velocity = 9.4×10^{-4} m./sec. The

Fig. 9

In Fig. 8 auxiliary lines have been drawn from various points on the operating line to the equilibrium line at an inclination of $k_L/k_G = 0·047$; the perpendicular of each triangle represents the driving force in the gas phase.

In the right hand half of Fig. 8 the reciprocal value of the driving force has been plotted versus p_G. In this manner the number of transfer units has been found $N_G = 5·15$. For an $(H_t)_G = 3·2$ m of the packing given the packed height becomes 16·5 metres.

infed liquid contains 0·794 moles NaOH per litre and 0·0105 moles Na_2CO_3 per litre.

In Fig. 9 the operating line has been drawn for the above conditions. As the CO_2-vapour tension of the liquid is immeasurably low, throughout the apparatus, there is no equilibrium line.

By means of the formulae mentioned before it can be calculated that : $k_G = 1·05 \times 16^{-3}$ kg moles/(sec) (m²) (at.) and $k_L = 7·75 \times 10^{-5}$ m/sec.

In the manner outlined $\dot{n}$ can be calculated for various points of the operating line. The table provides a survey of the values found.

p_G at.	$\dfrac{B_L}{zA_i}$	$\dfrac{(kDB_L)^{\frac{1}{2}}}{k_L}$	$\dfrac{\dot{n}}{k_LA_i}$	$\dot{n}$ kg moles/ (sec.) (m^2)	p_G-p_i at.
$1{\cdot}4\times10^{-2}$	1100	35	35	$0{\cdot}99\times10^{-6}$	$0{,}094\times10^{-2}$
2·0	620	32	32	1·30	0·124
2·55	400	29	29	1·51	0·144
3·4	190	23	23	1·63	0·122

By means of the graphical integration carried out in the right-hand half of Fig. 9 we find $N_G = 21$.

When using the above value of $k_G = 1{\cdot}05 \times 10^{-3}$ and assuming that the active area a per unit volume of the rings used is equal to 430 m^2/m^3 (= total surface area), it follows from formula : $N_G = \dfrac{k_G\,RT\,a\,h}{u_g}$ that the height $h = 0{\cdot}45$ m.

In this example the chemical reaction is always the rate-determining factor. In Fig. 9 the customary rectangular triangles have been drawn of which $p_G - p_i$ forms the perpendicular and B_L the base. For the purpose of comparison the inclination k_L/k_Gz, being much steeper than the hypotenuses of the triangles has also been plotted in Fig. 9.

(c) *The absorption of carbon dioxide in ammonia. Likewise a moderately fast reaction*

From a gas mixture containing 20 per cent-by volume of carbon dioxide 90 per cent of the latter has to be removed by bringing the gas into contact with ammonia (fresh liquid contains 2 moles of NH_3 per litre and no CO_2) at a pressure of 10 at. and a temperature of 20°C.

The superficial gas velocity in the column to be used is 0·0183 m/sec., the superficial liquid velocity being 0·001 m/sec. The packing material consists of 1 in. Raschig rings.

The operating line for the situation given has been drawn in Fig. 10. The CO_2-vapour tension may be neglected throughout the apparatus, so that the equilibrium line is absent. Values for k_G and k_L have been calculated and amount to : $k_G = 8{\cdot}0 \times 10^{-5}$ kg moles/(sec) (m^2) (at.)

and $k_L = 6{\cdot}8 \times 10^{-5}$ m/sec. Now $\dot{n}$ may be calculated for several points of the operating line in the manner outlined.* The following table gives a survey of the values found.

p_G at.	$\dfrac{B_L}{zA_i}$	$\dfrac{(kDB_L)^{\frac{1}{2}}}{k_L}$	$\dfrac{\dot{n}}{k_LA_i}$	$\dot{n}$ kg moles/ (sec.) (m^2)	p_G-p_i at.
2·0	1·4	4·45	2·1	$1{\cdot}03\times10^{-5}$	0·129
1·4	6·9	10·2	5·8	1·8	0·225
1·1	14·7	12·5	8·8	2·0	0·25
0·78	26	15	12	1·8	0·225
0·2	240	20	20	0·63	0·079

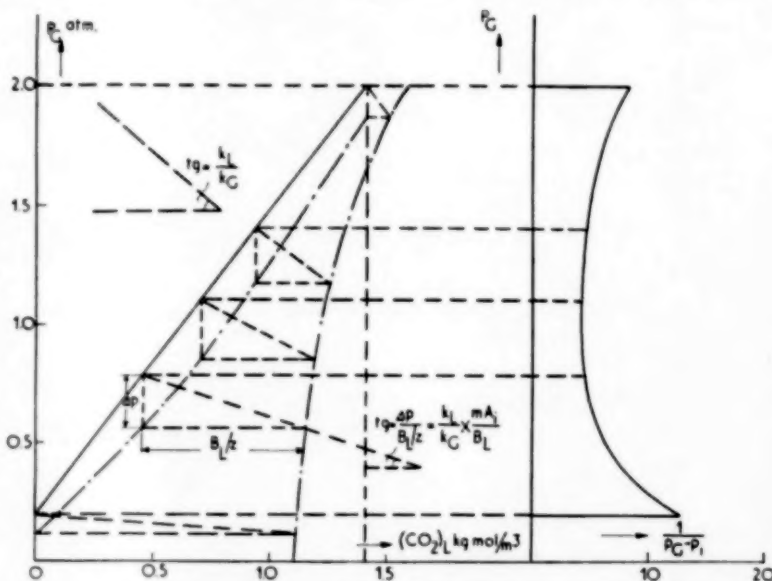The values found for $p_G - p_i$ are shown in Fig. 10. The graphical integration has again been carried out in the

Fig. 10

right-hand half of the figure and yields the number of transfer units : $N_G = 10$. When $H_{tG} = 1$ ft, the height of the column must be 10 ft.

By way of illustration the customary rectangular triangles have been drawn in Fig. 10, their perpendiculars representing the driving force in the gas = $p_G - p_i$. As the value of z varies from point to point, B_L/z has been

* z varies with the ammonia concentration of the solution. In a dilute solution NH_4HCO_3 is formed so that $z = 1$. In a concentrated solution, however, $NH_4NH_2CO_2$ (ammonium carbamate) is formed so that $z = 2$. In the intermediate concentration range z varies from 1-2 [11].

plotted along the horizontal axis. If the rate of the process is determined by transport of component B to the phase boundary, the inclination of the hypotenuse must be equal to k_L/k_G; this inclination is indicated in the figure. In correspondence with the table it appears that at the highest values of p_G the transport of B is indeed the determining factor, whereas at lower values of p_G the inclination decreases continuously so that the rate of the process becomes dependent on the reaction rate.

DISCUSSION

The method outlined above for the design of apparatus in which absorption combined with chemical reaction occurs, is liable to two important objections :

1. May the functional relationship between the three dimensionless products as derived be applied to technical apparatus, e.g. packed towers, in which the film-concept most likely does not correspond to actual conditions ?

2. How can the actual contact area—or the value of H_{TG}—be predicted for technical apparatus?

The first point has already been discussed on applying the relationship to experimental data of a batch apparatus and a wetted-wall column. For both apparatus good agreement was obtained. It is not known how flow conditions in packed columns differ from those in a wetted-wall column, but some analogy may be expected. Therefore, the authors assume that the method may be applied successfully to packed towers.

In any case, the deviations due to this point are expected to be small as compared with the uncertainty of the wetting of a packed column.

Through a number of articles it has become clear that the active area of a packed column is only a fraction of the total area of the packing material. For instance, the conditions given in example (b) correspond to an experiment carried out by Tepe and Dodge [8] (Test No. 2). Calculation leads to a column height of 0.45 m., under the assumption that the whole packing material was active. In the experiment, the actual column height was 2.3 m. It may be concluded that the effective area is only about 20 per cent of the total area.

In the above calculation it is implicitly assumed that the liquid was homogeneously distributed over the wetted part of the surface. In how far also this assumption is correct is still unknown. However, there is reason for expecting that in many cases the distribution over the packings is anything but homogeneous as was pointed out already by Gilliland [2]. Probably, the distribution will be less homogeneous according as the irrigation is less complete.

Suppose that under given conditions a liquid in viscous flow is homogeneously distributed over the contact surface, forming a layer of liquid of a constant thickness y and a constant mean velocity u_L. If on the other hand 90 per cent of the liquid flows over 10 per cent of the surface area, i.e. 9 times as much liquid per wetted perimeter, the thickness of the layer in that area becomes $(9)^{\frac{1}{3}} y = 2 \cdot 1 y$; the velocity, however, becomes $(9)^{\frac{2}{3}} u_L = 4 \cdot 3 u_L$. The original absorption rate being $\dot{n}$, the absorption rate on 10 per cent of the surface area will become $(4 \cdot 3)^{\frac{1}{2}} \dot{n} = 2 \cdot 65 \dot{n}$ if transport in the liquid phase determines the absorption rate. The remaining 90 per cent of the surface is wetted by 10 per cent of the liquid ; the absorption rate for this part, calculated in the same way, amounts to $0 \cdot 375 \dot{n}$. For the mean absorption rate over the entire area we thus find $0 \cdot 60 \dot{n}$.

Now the thickness of the liquid layer in the poorly wetted part is $0 \cdot 48 y$, so that at first sight one might think that the entire area were well wetted.

If in the same apparatus an absorption process should be carried out, the rate of which were exclusively determined by a resistance in the gas phase, the entire area would take part in the process for the full 100 per cent. This holds also for an absorption with chemical reaction where the chemical reaction rate is the determining factor of the process. For in this case $\dot{n} = A_i (kDB_L)^{\frac{1}{2}}$, so that it is independent of k_L. The phenomenon of a non-uniform liquid distribution makes it difficult therefore to make a comparison between different absorption processes carried out in the same packed column.

Non-uniform irrigation becomes particularly detrimental when two components must be selectively absorbed from a gas mixture, e.g. the absorption of CO_2 and H_2S in a soda solution.

Though the reaction rate of H_2S is greater than that of CO_2, the absorption of H_2S depends on k_L, whereas the absorption of CO_2 does not depend on this factor. Non-uniform irrigation causes a decrease in the absorption rate of H_2S, but does not affect the absorption rate for CO_2. This implies that the absorption of CO_2 is favoured with respect to that of H_2S, or in other words, the selectivity of the process decreases.

A better understanding of the mechanism of the irrigation of a packed column is an essential preliminary to the designing of these apparatus, in particular for processes in which gas-liquid reactions occur.

As long as further data on this subject are not available, the only way for the design of gas-liquid reactors is making two assumptions, viz. :

1. That the functional relationship given here does hold.
2. That H_{TG} is a constant for a given apparatus and that for chemical absorption its value is the same as for physical absorption.

LITERATURE

[1] DANCKWERTS, P. V.; Ind. Eng. Chem. 1951 **43** 1460. [2] GILLILAND, E. R.; Chem. Eng. Progress, 1951 **47** (No. 1) 11. [3] HITCHCOCK, L. B.; Ind. Eng. Chem. 1934 **26** 1158. [4] LANGHAAR, H. L.; Dimensional Analysis and Theory of Models, J. Wiley & Sons 1951. [5] SAAL, R. N. J.; Thesis Amsterdam 1927, Rec. Trav. Chim. 1928 **47** 73 264. [6] SHERWOOD, T. K. and HOLLOWAY, F. A. L.; Trans. Amer. Inst. Chem. Engrs. 1940 **36** 39. [7] SHERWOOD, T. K. and PIGFORD, R. L.; Absorption and Extraction, McGraw-Hill Book Co., 2nd Ed. 1952. [8] TEPE, J. B. and DODGE, B. F.; Trans. Amer. Inst. Chem. Engrs., 1943 **39** 255. [9] VAN KREVELEN, D. W., HOFTYZER, P. J. and VAN HOOREN, C. J.; Rec. Trav. Chim. 1948 **67** 133. [10] VAN KREVELEN, D. W. and HOFTYZER, P. J.; ibid. 1948 **67** 563. [11] VAN KREVELEN, D. W. and VAN HOOREN, C. J.; ibid., 1948 **67** 587. [12] VAN KREVELEN, D. W. and VAN HOOREN, C. J.; Chim. et Ind. XXIe Congrès Intern. Chimie Ind. 1948 p. 166. [13] VAN KREVELEN, D. W. and HOFTYZER, P. J.; ibid., p. 168.

NOTATION

A = concentration of component A — kgmol/m³
a = effective interfacial area per unit volume — m²/m³
a_p = total area of packings per unit volume — m²/m³
B = concentration of component B — kgmol/m³
D = coefficient of diffusion — m²/sec.
H = coefficient of Henry — kgmol/(m³)(at.)
H_t = height of a transfer unit — m
h = height of column — m
k = reaction rate constant — m³/(sec.)(kgmol)
k_G = coefficient of mass transfer in gas — kgmol/(sec.)(m²)(at.)
k_L = coefficient of mass transfer in liquid — m/sec.
m = multiplication factor
N = number of transfer units
$\dot{n}$ = rate of mass transfer per unit surface — kgmol/(sec.)(m²)
p = partial pressure — at.
R = gas constant — m³ at./(kgmol) (°K)
T = absolute temperature — °K
u = superficial fluid velocity — m/sec.
x_L = effective liquid film thickness — m
z = number of moles B reacting with 1 mole A
μ = viscosity — kg/(m) (sec.)
ρ = density — kg/m³
Γ = liquid rate per wetted perimeter — kg/(m) (sec.)

Subscripts :
G = gas phase
i = at the interface
L = liquid phase

Indices :
o = for the fluid entering the column
e = for the fluid leaving the column

All dimensions are expressed in the MKS Mass system.

The effect of surface active agents in liquid extraction processes

F. H. GARNER AND A. R. HALE

The Chemical Engineering Department, The University, Birmingham, 15

Summary—In liquid-liquid extraction processes where mass transfer takes place between droplets and a continuous liquid phase, the presence of trace quantities of surface active materials is shown to have a marked effect on the rate of transfer. On addition of only 0·015 per cent of *Teepol* to the water phase, the rate of extraction of diethylamine from toluene drops by water is reduced to 45 per cent of its original value.

The presence of adsorbed molecules at the interface reduces the rate of mass transfer from drops which do not circulate and also retards internal circulation in circulating systems.

Résumé—Dans les opérations d'extraction entre phases liquides ou le transport matériel s'effectue entre une phase liquide continue et des gouttelettes, la présence de traces d'agents tensio-actifs a une influence considérable sur la vitesse d'échange. Par addition de *Teepol* à la phase aqueuse, en quantités ne dépassant pas 0·015 per cent, on réduit de 45 per cent la vitesse d'extraction de la diéthylamine contenue dans des gouttes des toluène

La présence de molécules adsorbés sur l'interface réduit la vitesse d'échange pour des gouttes à l'intérieur desquelles n'existe pas de circulation. Elle retarde ce mouvement de circulation lorsqu' il existe dans les gouttes.

In recent years considerable advances have been made toward the better understanding of the mechanism of mass transfer from liquid drops and of factors influencing the rate of mass transfer in liquid-liquid extraction processes. SHERWOOD, EVANS and LONGCORE [1] found that the rate of extraction of acetic acid from benzene drops by water was far in excess of that predicted by theoretical relations for mass transfer by molecular diffusion. They concluded that this was due to movement of the fluid within the drop which maintained a higher concentration gradient at the interface than would exist if the interior were stagnant. Further data obtained on this system by WEST, ROBINSON, MORGENTHALER, BECK and McGREGOR [2] show lower rates of extraction than those of SHERWOOD and it was concluded that in this case the interiors of the drops were stagnant, due to the presence of trace quantities of plasticizer extracted from *Tygon* tubing in the benzene feed line.

GARNER [3], and GARNER and SKELLAND [4] have demonstrated this internal circulation by suspended coal particles and colour reactions in the drops for systems of low interfacial tension when diffusion is taking place. It has been estimated by KRONIG and BRINK [5] that the rate of

mass transfer from a drop when the continuous phase resistance is negligible will be increased by a factor of 2·5 when the interior circulates, hence the presence or absence of this circulation will have a profound effect on the efficiencies of commercial extraction equipment where the transfer is taking place between drops and a continuous phase.

Adsorbed films and circulation

For drops having an interfacial tension between the drop and continuous phases of about 1 dyne/cm GARNER and SKELLAND have shown that a toroidal circulation is set up within the drop provided the Reynolds number exceeds a well defined value known as the critical Reynolds number, and at Reynolds numbers below this value the interior is stagnant and any suspended particles merely sediment towards the base. Their work was confined to systems in which mass transfer was taking place and with very low interfacial tensions, they did show, however, that as the interfacial tension increased from 1 to 5 dynes per cm, the critical Reynolds number increased from 70 to 120.

BOND and NEWTON [6] from an experimental study of the velocity of air bubbles and mercury

drops in viscous media deduced that the radius of the smallest drop or bubble in which circulation takes place is given by the relation

$$r = \left(\frac{\gamma}{(\rho_1 - \rho_2) g} \right)^{\frac{1}{2}}$$

where r is the critical radius, γ the interfacial tension, ρ_1 and ρ_2 the densities of the inner and outer phases and g the acceleration due to gravity. This relation was based on experimental data in the streamline region with Reynolds numbers less than unity and is therefore not generally applicable in chemical engineering problems where the transition usually takes place at much higher Reynolds numbers. For nitrobenzene drops falling through water a critical diameter of 0·7 cm is predicted which is far above the observed value.

The motion inside drops of nitrobenzene has been studied by suspending fine aluminium particles in the drops and observing them while falling through water in reflected light. The drops were formed by injecting a small quantity of the suspension into a capillary tube by means of a side tube, its volume could then be measured. The drop was then ejected into a column of water from the open end of the capillary tube which was flared to permit the free release of the drop. The water used to eject the drop was the same as that contained in the column.

It was found that internal circulation is not restricted to systems where mass transfer is taking place and the transition from stagnant to circulating conditions is not sharp. In small drops slight movement near the leading pole of the drop was observed and as the diameter was increased circulation in the drop gradually became more complete, extending towards the rear of the drop until the whole of the interior was circulating. The transition from stagnant to completely circulating conditions takes place over a two-fold increase of diameter.

The effect of the addition of small quantities of a surface active agent, *Teepol*, to the water phase on the critical diameter of nitrobenzene drops has been investigated. The critical diameters at which circulation began are recorded in Table 1 and represent the smaller diameter in which any movement is detectable.

The critical diameter is increased by the addition of very small quantities of *Teepol* so small that the interfacial tension is not altered as measured by the drop weight method.

Table 1.

Concentration Teepol % by vol.	Interfacial Tension dynes/cm	Critical Diameter, cm
0		
0·000075	25·3	0·21
0·00015	25·3	0·23
0·0003	25·3	0·26
0·0006	25·3	0·36
0·0012	25·0	0·48
0·0024	24·2	0·50
0·0048	22·8	above 0·6

The critical diameters at *Teepol* concentrations greater than 0·0045 per cent by vol. could not be determined because it was found impossible to produce drops large enough by this method.

It is apparent that trace quantities of surface active agents form an adsorbed layer on the surface of nitrobenzene drops which acts as a quasi-rigid structure at the interface and prevents the transmission of shear across it. In extraction processes in which the interiors of the drops circulate under normal conditions the presence of trace quantities of surface active agents will cause a marked decrease in the rate of transfer due to this hindrance of circulation.

Adsorbed films and diffusion

CHU, TAYLOR and LEVY [7] reported that a reduction of interfacial tension from 24 to 2 dynes/cm by the addition of a surface active agent reduced the HTU of a packed liquid-liquid extraction column by about 50 per cent, and the addition of further quantities showed some tendency to decrease the efficiency. The effect of the agent on the rate of transfer across the interface is, however, masked by the increase in the mass transfer area. It is probable that the rate of transfer is reduced but this is more than counterbalanced by the increase in area.

FARMER [8] reports data on the effect of addition of *Tergitol* No. 4 and No. 7 on the rate

of extraction of acetic acid from single drops of carbon tetrachloride by water and concludes that the effect is no more than would be expected by the reduction in the size of the drops. Examination of his data however reveals that there is first a decrease in the percentage of equilibrium attained and then an increase as the quantity of agent present is increased. An increase would be expected to occur with increased concentration due to the reduction in the size of the drops.

This tendency appears to have been considered negligible by Farmer. The carbon tetrachloride acetic acid-water system has a high interfacial tension and is likely to be non-circulating.

The effect of the addition of various alcohols on the rate of extraction of acetic acid from benzene drops by water has been investigated by West, Herrman, Chong and Thomas [9] who show that the addition of several percent of some alcohols increases the rate of extraction. It is unlikely that the phenomenon observed is precisely the same as that when highly surface active molecules are present in view of the much higher concentrations required in the former case.

Gordon and Sherwood [10] have studied the effect of several surface active agents on the rate of transfer of n-butyric acid from water to benzene in a cylindrical vessel. Each phase was stirred by a stirrer with two vanes which did not disturb the interface to any appreciable extent. They conclude that surface active agents do not affect the rate of transfer and interfacial barriers hindering the passage of the solute through the interface are not set up.

Further examination of Gordon and Sherwood's data reveals a similar trend to that in Farmer's, the overall coefficient first decreases and then increases as the concentration of the surface active agent is increased. This is evident with three of the agents used, *Ultrawet*, *Aerosol O.T.* and *W70*. With *Santomerse D* there is a steady decrease in the overall coefficient as the interfacial tension is reduced from 24 to 4 dynes/cm. The concentrations at which the minimum overall coefficients are observed are shown in Table 2.

Hutchinson [11] carried out experiments in an apparatus similar to that used by Sherwood

Table 2.

Agent	Concentration	Overall Coefficient cm/hr	Interfacial dynes/cm
None	—	1·37	
Ultrawet	0·005 vol. %	1·26	16·5
Aerosol O.T.	0·002 wt. %	1·02	12·5
W. 70	0·0045 wt. %	1·00	11
Santomerse D	0·06 wt. %	1·13	4

and Gordon and concludes that when a surface active agent is present there may be some interaction of the solute and the surface film which retards diffusion. The transfer of various solutes from water to benzene in the presence of sodium cetyl sulphate was investigated. The rates of diffusion of n-butyl alcohol and n-butyl amine were greatly retarded, but much less effect was shown with ether or methyl ethyl ketone as solutes, indicating that the presence of hydrophilic groups increase the retardation. Experiments were carried out with films of other agents and in all cases a similar retardation was evident. He also found that in the presence of sodium cetyl sulphate there was a considerable retardation with n-amyl alcohol but practically no effect with tertiary amyl alcohol.

The retardation was not proportional to the surface pressure, and the greatest relative retardations occurred at low surface pressures with very small concentrations. The effect is therefore not due solely to the interface being blocked with large molecules with a corresponding reduction in the area available for mass transfer.

An analogous process to this resistance to diffusion across a liquid interface is the resistance to evaporation offered by monomolecular films on water.

Rideal [12] was unable to detect any retardation in the rate of evaporation of water from an open dish when covered with a monomolecular layer of stearic acid or oleic acid. However, in an inverted U tube under vacuum with one leg at 0°C and the other at 25°C the rate of evaporation was reduced by about 25 per cent by stearic acid and 50 per cent by oleic acid.

Langmuir and Langmuir [13] found the rate

of evaporation from a water surface in a wind of about 180 cm per second to be reduced by half by a film of cetyl alcohol, but fatty acids showed no effect.

SEBBA and BRISCOE [14] found that the resistance offered by surface films is a highly specific property. Egg albumin, cholestrol, oleic acid and elaidic acid offered practically no resistance under any conditions whereas stearic acid, brassidic acid, arachidic acid, cetyl alcohol, octadecyl alcohol and n-docosonol under suitable conditions can reduce the rate of evaporation of water considerably. The resistance became substantial only after the surface film had been compressed and the critical surface pressure exceeded. Hydrophilic groups tended to reduce the resistance and an increase in the length of the hydrocarbon chain increased it. Later work by SEBBA and SUTIN [15] confirmed their observations on cholestrol although HUTCHINSON reports that cholestrol does present a resistance to diffusion across a liquid-liquid interface.

LANGMUIR and SCHAEFER [16] studied the effect of monolayers of organic acids on the rate of evaporation from a free water surface taking special precautions to eliminate errors due to convection above the liquid surface. All the acids investigated presented a resistance which increased with the surface pressure. Experiments with cholestrol showed that it does present a small resistance indicating that the methods used by SEBBA and BRISCOE and SEBBA and SUTIN are not precise enough to detect it. It was also found that the pH of the water has a significant effect on the resistance of the film.

Data are presented in Table 3 showing the effect of small additions of *Teepol* on the rate of extraction of diethylamine from toluene drops by water, *Teepol* being added to the water phase. The toluene was fed at the base of a column of water 99 cm long and 2 in. diameter, through a single jet. All experiments were carried out at 20°C. The top of the column was conical with the outlet of 1 mm capillary tube at the apex, the flow through this being regulated by a tap. The drops reaching the top were removed immediately by the tap which was manually controlled in order to reduce extraction at this point to a minimum. In each experiment about 10 ml. of the 5 per cent solution of diethylamine was passed through the column, the feed and raffinate being analysed by titration against hydrochloric acid solution.

The interfacial tension of the solution of *Teepol* against the 5 per cent diethylamine solution in toluene have been estimated by the drop weight method at a drop formation time of 5 seconds. This method does not give an absolute value for the interfacial tension since the composition of the two phases vary with time and also the concentration of the surface active agent at the interface. The method, however, enables the conditions for each determination to be made identical. Attempts were made to measure interfacial tensions by the ring method but this was found to be unsatisfactory as the denser aqueous phase is drawn up by the ring and rupture of the interface takes place between the two outside films instead of between the inner and outer films. Considerable disturbance of the interface also occurs during the determination and the

Table 3.
Experimental data

Run No.	Concentration Teepol % by vol.	Drop Diameter (cm)	Rise secs.	Formation secs.	Initial concentration gm/litre	% Extracted	K cm/sec	γ dynes/cm.
2	0	0·462	9·8	2·1	34·2	46·8	0·0044	20·4
3	0·01	0·429	10·1	2·0	34·2	28·5	0·00213	16·3
4	0·02	0·400	10·7	2·0	34·2	30·0	0·00200	13·3
5	0·04	0·371	11·4	1·9	34·2	37·2	0·00228	10·7
6	0·06	0·353	11·5	2·0	34·2	37·0	0·00245	9·5
7	0	0·462	9·7	2·0	34·2	49·4	0·00482	20·4
8	0·004	0·447	9·6	2·0	34·2	27·0	0·00217	18·9

Fig. 1.

therefore
$$M = K \, 4\pi \left(\frac{3v}{4\pi}\right)^{2/3} \Delta C \int_0^{t_f} t^{2/3} \, dt$$

$$= K \, 4\pi \left(\frac{3v}{4\pi}\right)^{2/3} \frac{3}{5} t_f^{5/3} \Delta C$$

$$= 0\cdot6 \, K \, A_f \, t_f \, \Delta C$$

Hence for the determination of an average coefficient during formation the contact time must be multiplied by 0·6. Coefficients combining the formation and the rise have been calculated using a total time of $t_r + 0\cdot6 \, t_f$ where t_r is the time taken for the drop to rise through the water phase.
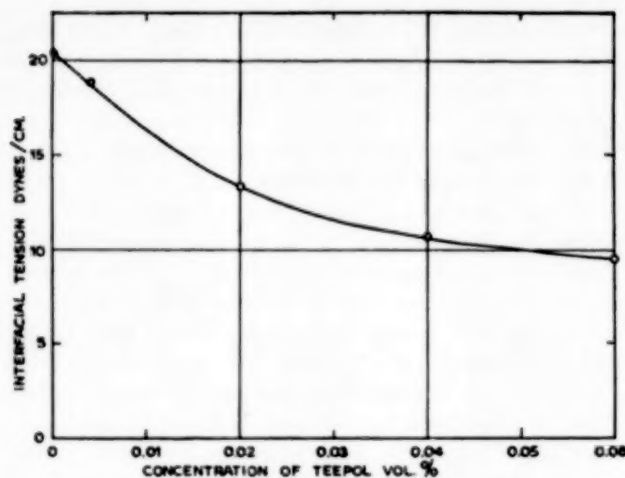
effective age of the film cannot be controlled.

The interfacial tensions between *Teepol* solutions up to 0·06 per cent by vol. and a 5 per cent solution of diethylamine in toluene are shown in Table 3 and Fig. 1.

In order to compare the rate of mass transfer from drops rising through solutions of a surface active agent it is necessary to calculate mass transfer coefficients. During the formation period the area is not constant and a correction can be made in the following way.

Assuming the mass transfer coefficient is constant during formation then the total material transferred during the growth of the drop (M) is given by

$$M = K \cdot \int_0^{t_f} A \, dt \, \Delta C.$$

where K is the mass transfer coefficient, A the surface area of the drop at time t, t_f the time of formation and ΔC the concentration driving force which may be assumed constant.

For a feed rate of v cc/sec. the area at time t is given by

$$A = 4\pi \left(\frac{3v}{4\pi}\right)^{2/3} t^{2/3}$$

Discussion of Results

The experimental data given in Table 3 and Fig. 2 show conclusively that the presence of a surface active agent in concentrations as low as 0·004 per cent may reduce the rate of extraction from liquid drops to a very marked extent. Observations with aluminium particles suspended inside the drops showed that the interior is stagnant when the continuous phase is pure water, hence this resistance to mass transfer cannot be due to a reduction in the intensity of circulation which would occur in a circulating system.

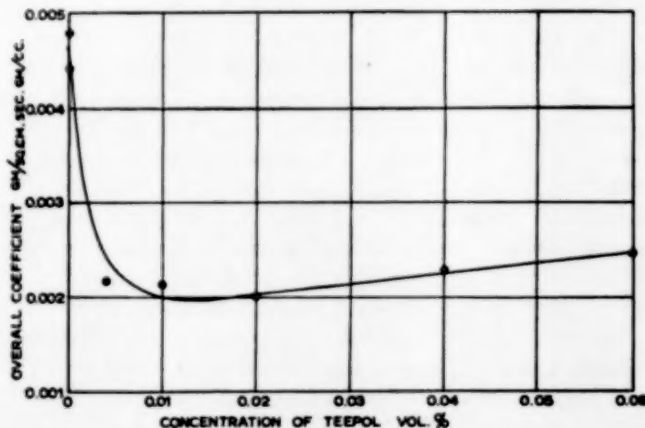As the concentration of the surface active agent

Fig. 2.

is increased, the mass transfer coefficient rapidly falls to a minimum and then increases steadily. The maximum resistance occurs at a concentration of 0·015 per cent, the increase in the coefficient at concentrations above this figure is probably due to the increased oblateness and amplitude of the oscillations of the drops caused by the lowering of the interfacial tension. Fig. 1 shows that the interfacial tension of the system falls from 14·2 to 9·5 dynes per cm. as the concentration of *Teepol* is increased from 0·015 per cent to 0·06 per cent.

It will be noted that the minimum value of the coefficient which is 45 per cent of that in pure water, occurs at a *Teepol* concentration of 0·015 per cent. when the surface pressure is approximately 5 dynes. *K* falls to 48 per cent of its original value when the surface pressure is only 2·5 dynes.

These data and those of FARMER, and GORDON and SHERWOOD show that surface active molecules adsorbed at a liquid-liquid interface may present an appreciable resistance to mass transfer. The magnitude of this resistance was found to be much greater in the toluene-diethylamine-water system than those investigated by the previous workers ; which may be due to differences both in the systems and in the surface active agents. HUTCHINSON found that the resistance is highly specific in its nature. The resistance to evaporation of water offered by monomolecular films also appears to depend to a large extent on the nature of the film.

The resistance offered to mass transfer by adsorbed films can be due to the reduction in area available for diffusion by the presence of the large molecules of the surface active agent at the interface and to adsorption of the solute at the interface creating a barrier through which the solute must pass. If the reduction in area is the major factor then the resistance will be proportional to the concentration at the interface. Fig. 1 shows that up to a concentration of 0·06 per cent there is a steady reduction in the interfacial tension and surface saturation is not attained in the range covered, hence there is a regular increase in the concentration of *Teepol* molecules at the interface. The free area will decrease steadily

as the concentration is increased from 0 to 0·06 per cent. From Fig. 2 it can be seen that the resistance to transfer does not increase steadily but reaches a maximum at 0·015 per cent when the surface concentration is far less than required for saturation. It is concluded, therefore, that the resistance to transfer is not primarily due to the area occupied by the surface active molecules but to adsorption of the solute on the surface film. The work of HUTCHINSON led to a similar conclusion. It is apparent that at a *Teepol* concentration of 0·015 per cent the rate of adsorption and desorption is approximately equal to the rate of transfer and further additions have little effect. At lower concentrations some of the solute is transferred without being adsorbed.

GORDON and SHERWOOD [10] have shown that the LEWIS and WHITMAN [17] " two film theory " (which assumes the two phases to be in equilibrium at the interface) is applicable to mass transfer between two liquid phases and the total resistance is equal to the sum of the two film resistances. The data presented here show that when a surface active agent is present there is a third resistance at the interface hence equilibrium at the interface cannot exist and the theory does not hold.

Conclusions

In liquid-liquid extraction processes where transfer takes place between drops and a continuous phase the presence of traces of surface active materials may have two effects. Firstly if the drops circulate under normal conditions this will be retarded or arrested, and secondly, the diffusion across the interface will be retarded due to interaction of the solute and the adsorbed surface active molecules. For a non-circulating system adsorbed films with surface pressures as low as 2·5 dynes/cm may reduce the rate of transfer by about 50 per cent.

REFERENCES

[1] SHERWOOD, T. K., EVANS, J. E. and LONGCORE, J. V. A.; Ind. Eng.Chem. 1939 **31** 1144. [2] WEST, F. B., ROBINSON, P. A., MORGENTHALER, A. C., BECK, T. R. and McGREGOR, D. K.; Ind. Eng. Chem. 1951 **41** 235. [3] GARNER, F. H.; Trans. Inst. Chem. Eng. 1950 **28** 88. [4] GARNER, F. H. and SKELLAND, A. H. P.; Trans. Inst.

Chem. Eng. 1951 **29** 315. [5] KRONIG, R. and BRINK, J. C.; Appl. Sci. Res. 1950 **A.2** 142. [6] BOND, W. N. and NEWTON, D. A.; Phil. Mag. 1928 **5** 794. [7] CHU, J. C., TAYLOR, C. C. and LEVY, D. J.; Ind. Eng. Chem. 1950 **42** 1157. [8] FARMER, W. S.; Oak Ridge National Laboratories, unclassified report O.R.N.L. 1950 635. [9] WEST, F. B., HERRMAN, A. J., CHONG, A. T. and THOMAS, L. E. K.; Ind. Eng. Chem. 1952 **44** 625. [10] GORDON, K. F. and SHERWOOD, T. K.; presented at Mtg. A. I. Chem. Eng. Toronto, April 1953 29. [11] HUTCHINSON, E.; J. Phys. & Coll. Chem. 1948 **52** 897. [12] RIDEAL, E. K.; J. Phys. Chem. 1925 **29** 1585. [13] LANGMUIR, I. and LANGMUIR, D. B.; J. Phys. Chem. 1927 **31** 1719. [14] SEBBA F. and BRISCOE, H.; J. Chem. Soc. 1940 106. [15] SEBBA, F. and SUTIN, N.; J. Chem. Soc. 1952 2513. [16] LANGMUIR, I. and SCHAEFER, V. F.; J. Franklin Inst. 1943 **235** 119. [17] LEWIS, W. K. and WHITMAN, W. G.; Ind. Eng. Chem. 1924 **16** 1215.

Hydroextraction VI : The effect of cake shape

M. M. Haruni and J. Anderson Storrow

Chemical Engineering Laboratory, Applied Chemistry Department, College of Technology, Manchester

Summary.—The flow of liquid through a wedge shaped cake has been studied theoretically and experimentally for filtration and hydroextraction. Approximate equations based on flow in the force field direction only have been compared to the relaxation solutions for flow rates. The use of a flow equation based on a uniform cake thickness equivalent to the mean of the wedge has been discussed.

Résumé—Etude théorique et expérimentale de l'ecoulement au travers d'un gateau en forme de coin, aussi bien pour la filtration que pour l'essorage. L'auteur compare l'equation précise de relaxation à des relations simplifiées (ecoulemente du liquide uniquement dans la direction du champ de forces). Discussion d'une equation basée sur l'emploi d'une epaisseur uniforme, équivalente à l'epaisseur moyenne du coin.

The drainage rate of wash water from a hydroextractor cake has been shown [1], [2], [3] to follow closely the equation :

$$q = \frac{4\pi^3 \, n^2 \, X \, K_c}{\mu g} \cdot \left[\frac{r_0^2 - r_L^2}{\log_e r_0/r_c} \right] \qquad (1)$$

based on the liquid flowing radially through the cake from an inner radius r_c to an outer radius r_0, the liquid surface being maintained constant at r_L with $r_L < r_c$. The face of the liquid may be assumed vertical without appreciable error [8]. Similarly the paraboloids of revolution representing surfaces of equal pressure at positions within the liquid between r_L and r_0 may be approximated closely by vertical cylindrical surfaces. The centrifugal head difference developed across such surfaces of an elemental annulus was equated to the resistance to liquid flow, leading to pressure distributions discussed earlier [7].

The cylindrical surfaces of equal pressure were considered in conjunction with cylindrical cakes. The equation above is based on cakes of vertical surface at radius r_c. It is not unusual to find that cakes do not conform to this shape. Since preparation of a cake surface to make it conform would be unwise with certain materials owing to the risk of varying the residual cake permeability, it is necessary to consider the effect of the cake shape on permeabilities estimated from the flow equation (1) or others based on it [3].

Cake shapes :

The shape of hydroextractor cakes will depend on various factors

(a) the physical properties of the cake material ; density, particle size, particle shape, and distribution of these properties,

(b) physical properties of the liquid ; viscosity, and notably surface tension in its effect on packing,

(c) geometry of the cake ; basket dimensions, cake dimensions, and packing of material in the cake,

(d) technique of cake formation ; basket speed, slurry concentration, feed rate.

The shape might be altered during the process of washing, especially at high speeds or high flow rates.

It has been found experimentally that the following will assist in the formation of a uniform vertical cake by feeding slurry to a spinning basket :

(a) avoiding high speeds during formation,
(b) avoiding the use of either high or low slurry concentrations,
(c) feeding at a high rate, keeping the cake surface completely submerged.

In tests with a 9 in. and 18 in. diameter hydroextractor [3], [6] starch slurries always tended to form vertical cakes. Even if a wedge-shaped cake is centrifuged under water, it quickly conforms to the vertical cylindrical shape with an insignificant variation in thickness. Cakes of starch could be
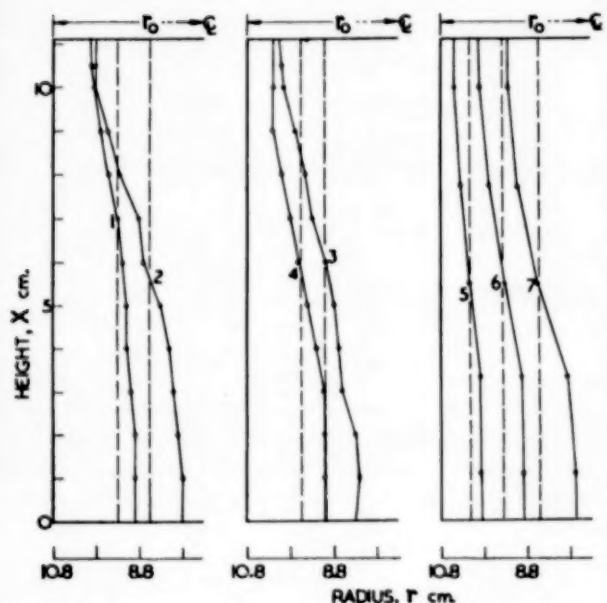
Fig. 1. Cross sections of hydroextractor cakes ; broken lines showing the mean radii.

easily formed to give a constant thickness within ± 1 mm, when observing the precautions mentioned above. Chalk and kieselguhr cakes often gave faces far from vertical. The face contours of cakes Nos. 1, 2, 3, 4 in Fig. 1 were measured using the probe technique [3], [6]. The data for cakes Nos. 5, 6, 7 were found [2] as mean values from five equal subdivisions of the length X of vertical sections of the cake. Although above precautions assist in forming a constant thickness cake, it is necessary to disturb slightly the liquid layer within the cake, i.e. between r_L and r_c with $r_L < r_c$, to distribute the cake material evenly. Although this procedure did not cause appreciable change in permeability with the present materials, it must be used with care. Barium sulphate, for example, will directly deposit at the bottom of the basket. It is impossible to form a vertical cake of this material without moulding the cake itself vigorously. It is thus necessary to analyse the flow mechanism through wedge cakes, and to decide whether approximate solutions may be obtained by assuming flow only in the direction of the force field, or even by neglecting the wedge-shape and considering the cake as of vertical face at a mean radius r_c.

FLOW RATE EQUATIONS

The complete solution for the flow relationships through a centrifuge cake with a sloping face will be complicated. The detailed description of the flow pattern should account for the wedge shape of the cake on any plane formed by a radius and the axis of rotation, the expanding cylindrical surface normal to the radial flow with increasing radius, and radial changes in permeability. It was considered satisfactory for the present purpose to check that the approximate forms shown below fulfilled certain conditions. The approximate equations account for the change in cylindrical area normal to the radius, but are based on the assumption that the flow through the wedge is radial and normal to the axis of rotation. The flow is not of this form but the main question is whether the difference between the true and laborious solution and the approximation introduces a complicating function. From the analyses mentioned below it appears likely that the approximation is small and thus can be used for consideration of variations of the flow rates with operating conditions.

Solution by Relaxation :

Consider two-dimensional flow of water through a wedge-shaped block of porous material, the liquid entering a face which is at an angle to the force field and leaving a face normal to the field. The term " wedge-shape " for hydroextractor cakes refers to the cake section on the plane formed by the axis of rotation and a radius, but not the section formed by a plane normal to the axis of rotation. The following solutions demonstrate flow of this type through filter cakes under hydrostatic pressure differentials and through hydroextractor cakes under centrifugally induced heads. The cases indicated in Fig. 2 have been assessed in each system, the cakes being uniform in permeability, with liquid level at LL and the flow being in the direction of the arrow carrying the acceleration appropriate to the force field, either "g" or "$r\omega^2$". The atmospheric pressure is taken as the zero datum at the level LL and at the drainage face CD. In all cases the cake is bounded by impermeable walls AD and BC. In the systems I, II, III, IV, V the cake face is taken as at $45°$ to the field direction to give a much greater possibility of divergence between the approximate and detailed solutions than

165

would occur in practice. In system VI the cake face AB is at an angle of $\tan^{-1} 0.5$ to CD and illustrates a practical case.
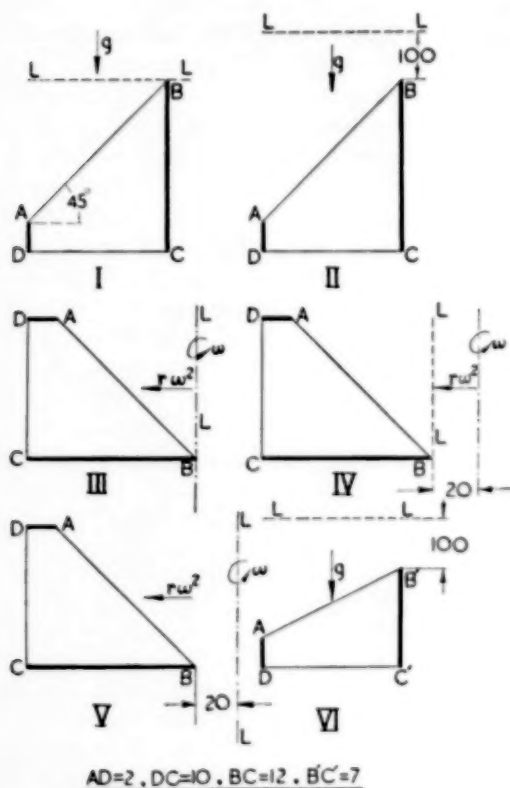

Fig. 2. Flow systems solved by relaxation.

In case I (Fig. 2) the flow occurs due to hydrostatic head of 12 cm water, i.e. from the level B to the drainage face, DC. In cases II, VI, the head is increased by 100 cm above B. The pressure distribution, p, in the liquid within the cake satisfies the following equations, u being the velocity along the x co-ordinate in the $ABCD$ plane in the DC direction, v being the velocity along a y co-ordinate in the AD direction, and the origin of co-ordinates being the meet of LL and DA :

$$\frac{\partial u}{\partial x} + \frac{\partial v}{\partial y} = 0 \tag{2}$$

$$-\frac{\partial p}{\partial x} - \frac{\rho g \mu}{K_F} \cdot u = 0 \tag{3}$$

$$-\frac{\partial p}{\partial y} - \frac{\rho g \mu}{K_F} \cdot v + \rho g = 0 \tag{4}$$

$$\nabla^2 p = \frac{\partial^2 p}{\partial x^2} + \frac{\partial^2 p}{\partial y^2} = 0 \tag{5}$$

The velocity potential ϕ defined as

$$\phi = -\frac{K_F}{\mu}\left(\frac{p}{\rho g} - y\right) \tag{6}$$

also satisfies the equation

$$\nabla^2 \phi = \frac{\partial^2 \phi}{\partial x^2} + \frac{\partial^2 \phi}{\partial y^2} = 0 \tag{7}$$

The flow may be assessed by the solution to the Laplace equation (5) or (7), which may be obtained from relaxation methods using the known pressure conditions along AB and CD, and the condition that $\frac{\partial p}{\partial x} = 0$ along AD and BC.

The centrifuge cases III, IV, V include a wide range of possibilities to test the effect of the cake position relative to the axis of rotation, and of the liquid level either maintained at B or the basket running full with $r_L = 0$. The equations in this case are modified by the centrifugal force acting in place of the gravitational field in cases I, II, VI and the gravitational field acting in the x direction. In addition to the continuity equation (2) the following must be satisfied, the origin of co-ordinates lying on the axis of rotation

$$-\frac{\partial p}{\partial x} - \frac{\rho g \mu}{K_c} \cdot u + \rho g = 0 \tag{8}$$

$$-\frac{\partial p}{\partial y} - \frac{\rho g \mu}{K_c} \cdot v + \rho y \omega^2 = 0 \tag{9}$$

$$\nabla^2 p = \frac{\partial^2 p}{\partial x^2} + \frac{\partial^2 p}{\partial y^2} = \rho \omega^2 \tag{10}$$

$$\phi^1 = -\frac{K_c}{\mu}\left[\frac{p}{\rho g} - x - \frac{y^2 \omega^2}{2g}\right] \tag{11}$$

$$\nabla^2 \phi^1 = \frac{\partial^2 \phi^1}{\partial x^2} + \frac{\partial^2 \phi^1}{\partial y^2} = 0 \tag{12}$$

For the experimental range considered in these papers the gravitational field has negligible effect on the flow pattern and the above equations may be simplified accordingly, the term containing gravitational acceleration being omitted from equation (8) and

removing "x" from equation (11). In the relaxation of $\nabla^2 p = \rho\omega^2$, it was found convenient to substitute $p' = \dfrac{2}{\rho\omega^2} \cdot p$ and so reduce the equation (10) to form $\nabla^2 p' = 2$, which is independent of centrifuge speed.

$ABCD$, may be found for any position y between A and D as

$$q' = \int_0^X \frac{\partial \phi}{\partial y} \cdot dx \qquad (13)$$

The slopes of curves $\dfrac{\mu}{K_F} \cdot \dfrac{\partial \phi}{\partial y}$ in Fig. 4 were taken at
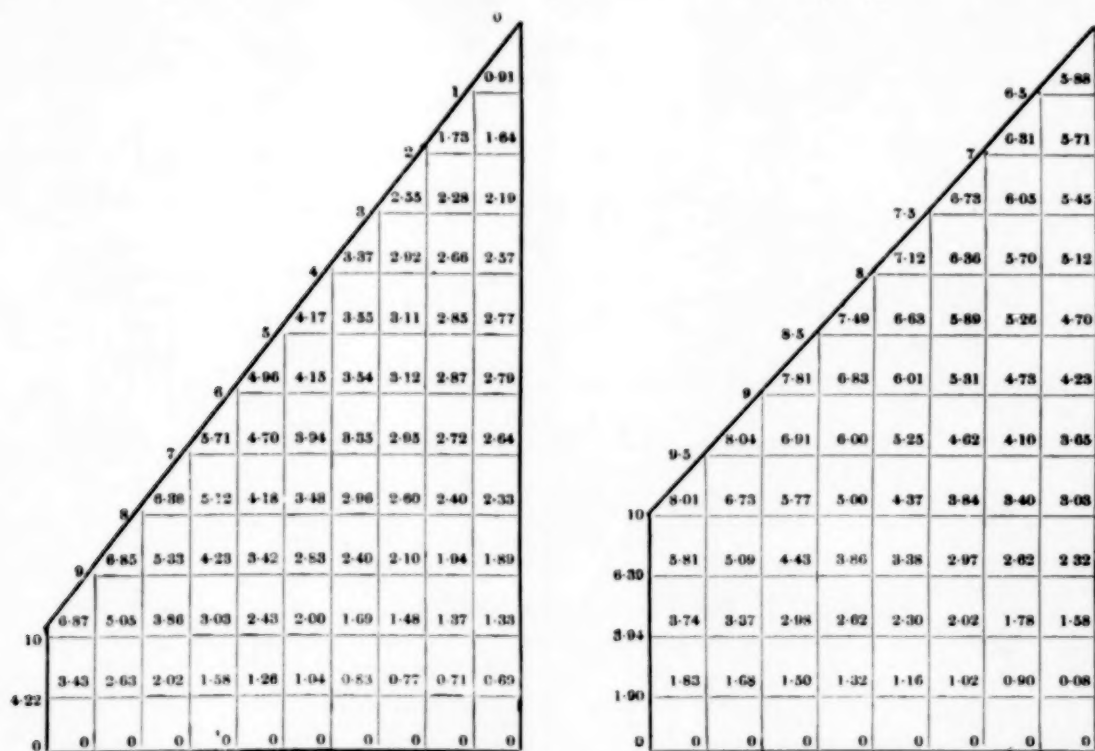
Left triangle (values):
```
                                    0
                                1  0·91
                              2  1·73  1·64
                            3  2·55  2·28  2·19
                          4  3·37  2·92  2·66  2·57
                        5  4·17  3·55  3·11  2·85  2·77
                      6  4·96  4·15  3·54  3·12  2·87  2·79
                    7  5·71  4·70  3·94  3·35  2·95  2·72  2·64
                  8  6·39  5·12  4·18  3·48  2·96  2·60  2·40  2·33
                9  6·85  5·33  4·23  3·42  2·83  2·40  2·10  1·94  1·89
              10 6·87  5·05  3·86  3·03  2·43  2·00  1·69  1·48  1·37  1·33
         4·22   3·43  2·63  2·02  1·58  1·26  1·04  0·83  0·77  0·71  0·69
                 0     0     0     0     0     0     0     0     0     0
```

Right triangle (values):
```
                                    3·88
                              6·31  5·71
                            7  6·73  6·05  5·45
                          7·5 7·12  6·36  5·70  5·12
                        8  7·49  6·63  5·89  5·26  4·70
                      8·5 7·81  6·83  6·01  5·31  4·73  4·23
                9·5 8·04  6·91  6·00  5·25  4·62  4·10  3·65
              10  8·01  6·73  5·77  5·00  4·37  3·84  3·40  3·03
         6·39  5·81  5·09  4·43  3·86  3·38  2·97  2·62  2·32
         3·94  3·74  3·37  2·98  2·62  2·30  2·02  1·78  1·58
         1·90  1·83  1·68  1·50  1·32  1·16  1·02  0·90  0·08
                 0     0     0     0     0     0     0     0
```

Fig. 3.   System I in Fig. 2 ; relaxation solution for $p/\rho g$.

Example of relaxation solution

The pressure distribution in Fig. 3 from equation (5) is quoted as head of fluid, $\dfrac{p}{\rho g}$, for the filtration case I in Fig. 2. In Fig. (4), $\left(y - \dfrac{p}{\rho g}\right) = \dfrac{\phi \cdot \mu}{K_F}$ is plotted against $(y - y')$. This plot was found more convenient than a plot against y and its grouping of curves for constant x. Each curve also had constant y' and thus led to a distribution of $\dfrac{\partial \phi}{\partial y}$ against y. The flow rate of q' from the drainage face DC for uniform unit depth of cake normal to the plane

$y = 11 \cdot 0$ cm and plotted against x in Fig. 5-I. The graphical integration of this distribution gave $\dfrac{\mu}{K_F} q^1$. Fig. 6 shows the flow path for case I with flow lines drawn perpendicular to the equipotential lines.

Approximate equations

If flow is assumed to occur only in the y direction, i.e. the field direction, in each case the following approximate flow equations may be solved far more readily than the more precise relaxation solutions. For the flow through the wedge under hydrostatic head H, taking unit depth normal to $ABCD$ (Fig. 7):
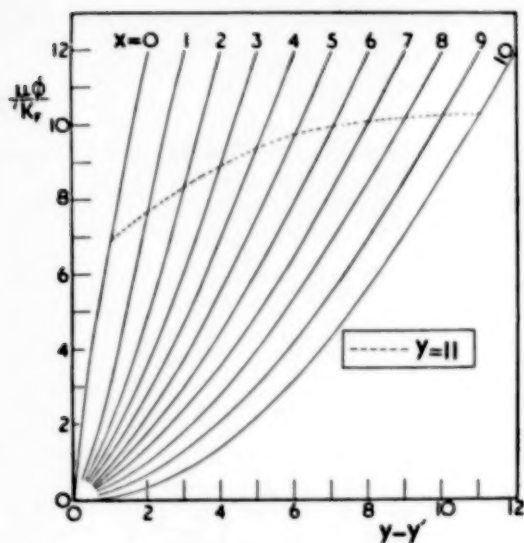
167

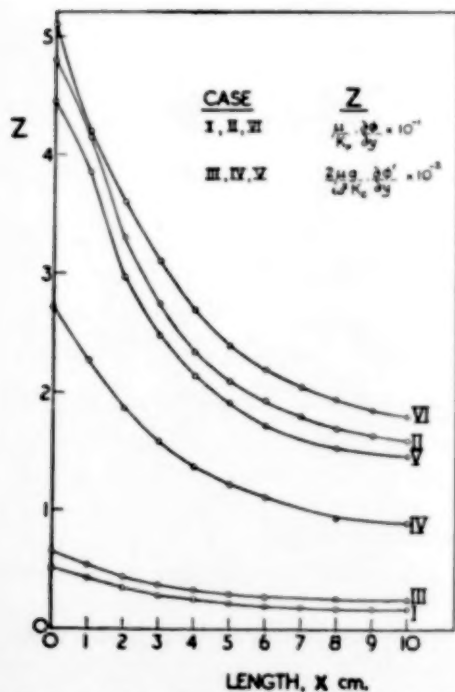Fig. 4. System I in Fig. 2. : distribution of velocity potential.

Fig. 6. System I in Fig. 2 : flow net.

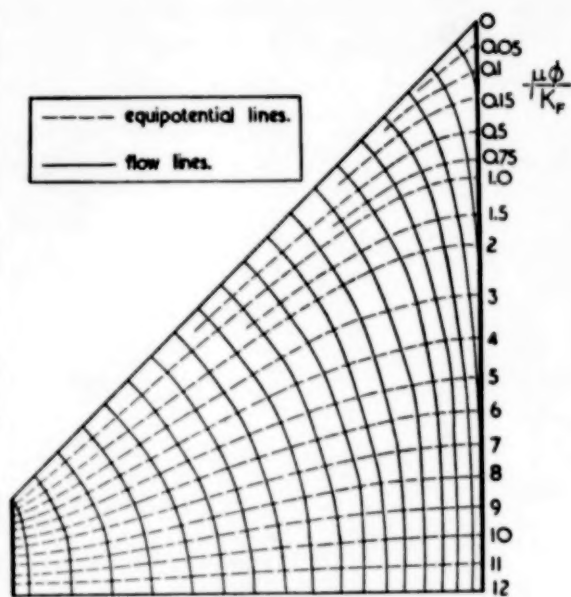Fig. 5. Systems I–VI in Fig. 2 : distribution of velocity potential gradients.
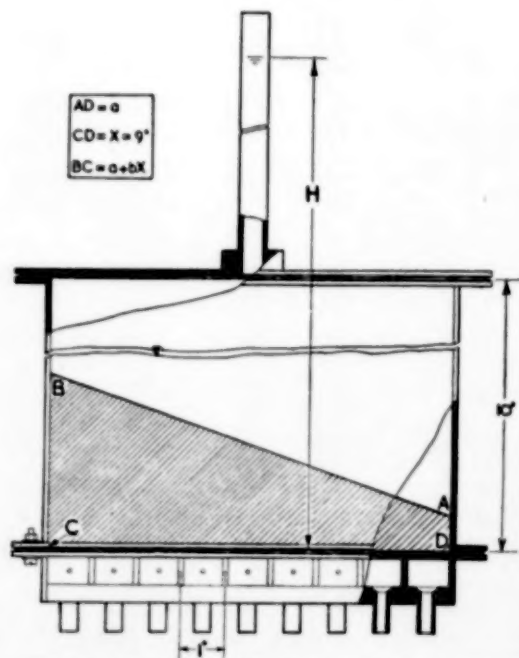
Fig. 7. Transparent filtration cell for flow segregation.

168

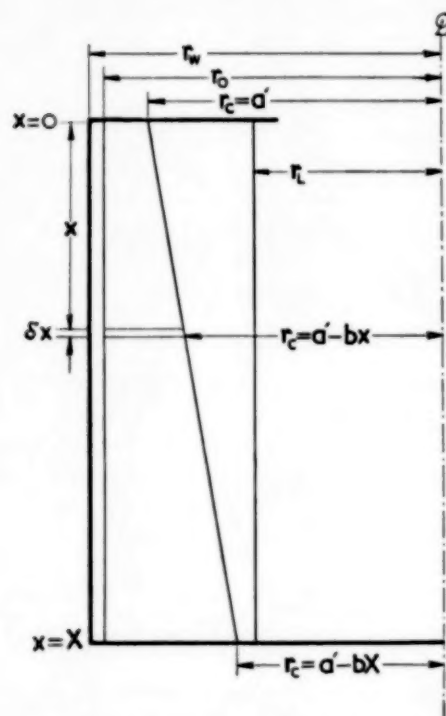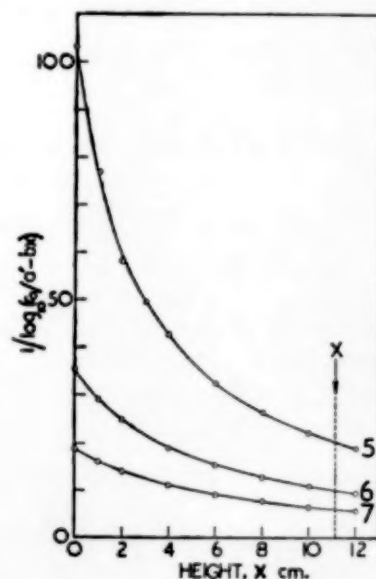By using the approximate method and taking into account the expanding cylindrical surface normal to the radial direction, it is to be expected that the approximations will not be far from the truth. Consider an elemental height δx of cake (Fig. 8) through which liquid flows at the rate δq. If pressure is assumed atmospheric at r_L and at r_0, and the cake has a permeability K_C,

$$dq'' = \frac{4\pi^3 n^2 K_c}{\mu g} \cdot \left[\frac{r_0{}^2 - r_L{}^2}{\log_e r_0/r_c} \right] \cdot dx \qquad (19)$$

If the permeability is assumed constant and the liquid surface taken as cylindrical, the flow rates from the whole cake are approximated by the integral form based on radial flow comparable to equation (18)

$$q'' = \frac{4\pi^3 n^2 K_c}{\mu g} \cdot (r_0{}^2 - r_L{}^2) \cdot \int_0^X \frac{dx}{\log_e \dfrac{r_0}{a' - bx}} \qquad (20)$$

The area below the appropriate curve of

Fig. 8. Wedge shape cake in hydroextractor.

$$dq'' = \frac{K_F H}{\mu . L} \cdot dx \qquad (14)$$

The path length L may be taken as $L = (a + bx)$ where length $AD = a$; length $BC = (a + bX)$. Then the total flow through the face DC is

$$q'' = \frac{K_F . H}{\mu . b} \cdot \log_e \frac{a + bX}{a} \qquad (15)$$

For a unit depth of cake normal to $ABCD$ operating under a centrifugal force (Fig. 8) the y co-ordinate may be taken as the usual r co-ordinate from the axis of rotation, the forces in equilibrium across an element of thickness dx being :

$$\frac{\omega^2}{2}\left(r_0{}^2 - r_L{}^2 \right) = \frac{\mu g}{K_c} \cdot \frac{dq}{dx} (r_0 - r_c) \qquad (16)$$

whence :

$$dq'' = \frac{\omega^2}{2g} \cdot \frac{K_c}{\mu} \cdot \left[\frac{r_0{}^2 - r_L{}^2}{r_0 - r_c} \right] dx \qquad (17)$$

$$q'' = \frac{\omega^2}{2g} \cdot \frac{K_c}{\mu b} (r_0{}^2 - r_L{}^2) \log_e \frac{r_0 - a' + bX}{r_0 - a'} \qquad (18)$$

where $a' = r_0 - AD$.

Fig. 9. Integrals for q'' in equation (20) ; for cakes 5, 6, 7 in Fig. 1.

$1/\log [r_0/(a - bx)]$ against x in Fig. 9 gives the required integral for the flow rate equations for a specific cake when taken between appropriate limits of x.

Accuracy of approximate equations

The ratio of q' from equation (13) to the approximate q'' from the appropriate equation (15) or (18) in the cases I, II, III, IV, V, VI (Fig. 2) has the values 1·20, 1·26, 1·31, 1·26, 1·24, 1·023 respectively. In the first five cases, where a 45° wedge is considered, the approximate equations lead to flow rates from 16 to 23% too low. The error is almost constant over a wide range of operating conditions in the two force fields and the centrifugal cases differ little from the hydrostatic head system. In case VI, where the sloping face is at an angle of $\tan^{-1}$ 0·5, the ratio q'/q'' was much lower and the approximate equations lead to flow rates only 2% lower than the true values. In practice, hydroextractor cakes would not be expected to have faces showing slopes higher than $\tan^{-1}$ 0·5 (Fig. 1) and the approximate equation (20) should lead to a reasonably accurate analysis.

Effect of neglecting wedge-shapes

The flow through a slab of width X, constant thickness L, and unit depth, under a hydrostatic head H, is given by

$$q = \frac{K_F . H . X}{\mu L} \qquad (21)$$

For the same slab of cake under centrifugal force :

$$q = \frac{\omega^2}{2g} . \frac{K_e X}{\mu} \left[\frac{r_0^2 - r_L^2}{r_0 r_e} \right] \qquad (22)$$

If the flow rate, q'', through a wedge is compared with the flow rate, q, through a slab of the same volume and permeability but of constant thickness, from equations (15, 21) for filtration :

$$\frac{q''}{q} = \frac{L}{bX} . \log_e \frac{a + bX}{a} \qquad (23)$$

and from equations (16, 22) for hydroextraction :

$$\frac{q''}{q} = \frac{r_0 - r_e}{bX} . \log_e \frac{r_0 - a' + bX}{r_0 - a'} \qquad (24)$$

In both cases, the ratio q''/q is 1·252 for $b = 1$ and 1·140 for $b = 0.5$, when $a = 2$ and $X = 10$. Thus, from the approximate flow rate equations, a cake of wedge shape allows a flow rate q'' higher than q for a constant thickness cake of same permeability and volume. The deviation is up to 25% when considering 45° wedges but is less than 14% in practical cases.

If the true flow rate q' from equation (13) is compared with the flow rate q from equations (21, 22) the results in Table 1 are obtained. While q' is more than 50% higher than q for 45° wedge, it is only 16% higher for the smaller slope of face.

<div style="text-align:center">Table 1</div>

angle of wedge	b	q'/q''	q''/q	q'/q
45°	1·0	1·25	1·25	1·56
26°36'	0·5	1·02	1·14	1·16

In hydroextractor cakes the cylindrical surface increases in the radial direction ; if the flow, q'', through a sloping-face cake is compared with the flow, q, through a vertical-face cake of the same volume and permeability, from equations (1, 20)

$$\frac{q''}{q} = \frac{1}{X} . \log_e \frac{r_0}{r_e} . \int_0^X \frac{dx}{\log_e \frac{r_0}{a' - bx}} \qquad (25)$$

The values of q''/q are 1·18, 1·12, 1·06 for the practical examples 5, 6, 7 in Fig. 1. These values are within
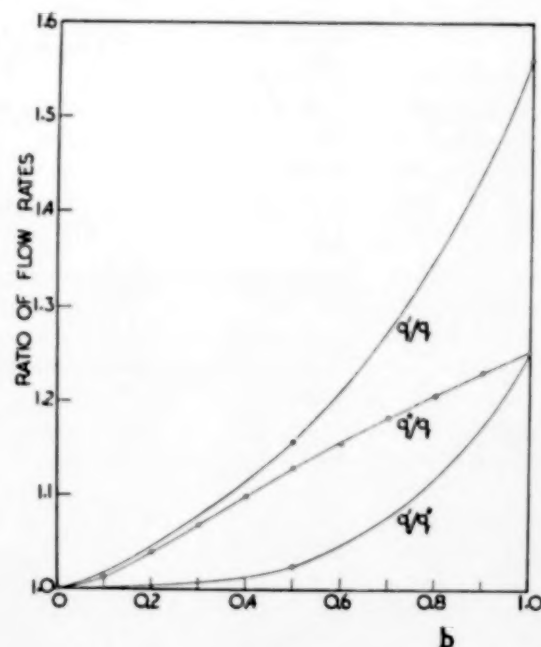

Fig. 10. Relationships of flow rates from equations (13, 18, 22).

the range obtained from comparing flow rates through slabs of similar slopes from equation (24).

From the above comparisons, a cake of wedge shape may allow a flow rate q' 50% higher than the flow rate q for a vertical cylindrical cake of same permeability and mean radius r_c but in practical cases, q' would be expected to be within 20% of q. Thus if equation (1) is used to analyse flow data from cakes of wedge shapes, the permeability calculated is expected to be about 20% higher than the true value. Fig. 10 shows the relationship between q, q' and q'' for different values of b.

Experimental investigations

In the study of flow rate distribution in filtration through a wedge-shaped cake, a *Perspex* cell (Fig. 7) was used to allow observation of cake formation and shape. The flows from sections of the outflow face were segregated by the dividing box below the cake
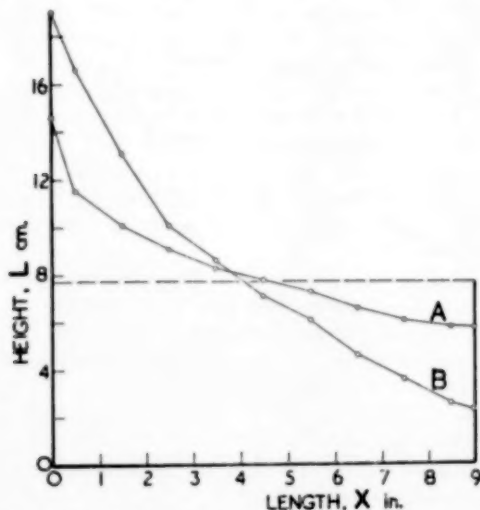
Fig. 11.   Face contours of cakes formed in filtration cell.

support. Cakes of maize starch, and of chalk were formed on one layer of twill cloth with the box in an inclined position to produce a sloping cake face. It is essential for the formation to occur with the cake completely submerged. The face contours in Fig. 11 were obtained by this method without vibration of the cell. To make straight faces of desired inclination (Fig. 12) it was essential to induce vibration. When the cake was suitably consolidated the box was
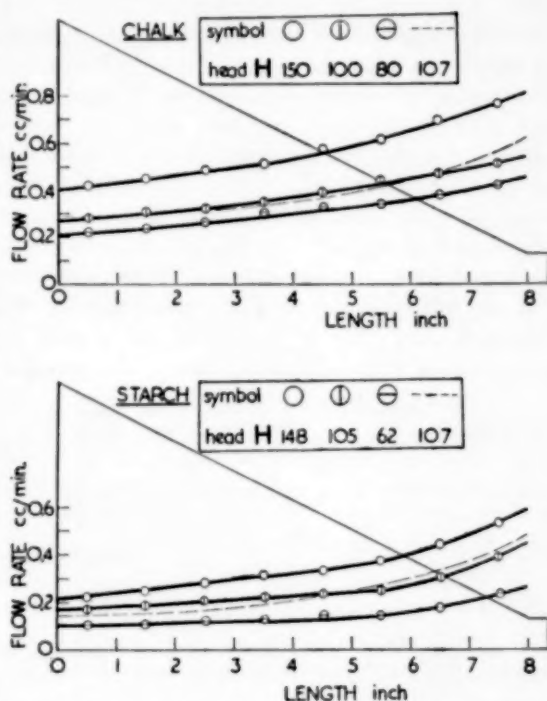
Fig. 12.   Flow distributions from wedge cakes in filtration cell ; the broken line being theoretical.

returned to its test position with the cake support horizontal. Water was fed to the closed box from heads up to 150 cm, and the segregated flow rates measured by collection of the drainage in calibrated 10 cc cylinders. The data in Fig. 12 for three heads on two cakes of inclination $\tan^{-1} 0.5$ show a ratio of total flow rate to head, and hence a permeability, constant to $\pm 1\%$. They also exemplify the agreement of form between the experimental results and the predicted distribution of the broken line from the relaxation analyses based on uniform permeability and $H = 107$ cm. This line was superimposed near the experimental data for $H = 100\text{–}105$ cm for comparison of form.

To study the effect of neglecting the wedge shape a kieselguhr cake was formed with constant thickness of 7·6 cm. After measuring the total filtration rate for the cake under a head of 20 cm water, the cake was disturbed to a slurry and reformed with the box in an inclined position. The cakes in Fig. 11 were obtained by this method without vibration. The box was returned to its normal position and the total flow

rate again measured under the same head. Finally the cake was reformed to constant thickness and tested again. The constant thickness cake gave flow rates of 20·0 cc/min initially and 19·6 cc/min finally, showing slight change in permeability throughout the test period. The non-uniform cakes in Fig. 11 gave rates of 22·0 and 23·0 cc/min for faces A and B respectively, i.e. q' was 12 to 17% higher than q for a uniform cake of the same volume. This agrees with the expected difference from Table 2.

Table 2

Cake No.*	Chalk Batch No.	Thickness of cake (cm)		Mean Permeability $K_e \times 10^7$ g/sec.^{2}		$\dfrac{q'}{q}$
		wedge max. min.	vertical	wedge	vertical	
1	1	1·9 0·9	1·50	2·96	2·37	1·25
2	1	3·0 1·0	2·20	3·10	2·38	1·30
3	2	2·6 0·8	1·80	1·90	1·40	1·35
4	3	1·8 0·6	1·23	2·68	2·07	1·29

*Cross-sectional diagrams of wedge cakes are shown in Fig. 1.

To assess the effect of neglecting sloping face forms in the hydroextractor, cakes of chalk of the same weight were made with vertical faces, as mentioned above, and also with sloping faces. The cake contours measured with the probe [3], [6] are shown in Fig. 1. The experimental data given in Table 2 were obtained from variations of r_L with time in drainage tests and of flow rate measurements at constant r_L [3].

The flow rates q' were 25–35% higher than q, as compared to 20% increase expected from equations (13, 20, 25). The higher increase may be due to the permeability distribution [6] in the wedge cake leading to increased flow through the thinner section of the cake. The effect of a minor unassessed factor is likely in that whereas the reproducibility of mean permeability K_e with vertical cakes was always good, the wedge reproducibility was inferior, e.g. being about 1% and 5% with cakes Nos. 1, 2 in Table 2. This variation is of the same magnitude as the excess increase in the q'/q ratio.

CONCLUSIONS

Experimental evidence has substantiated the opinion that the approximate equations based on flow in the force field direction only are sufficiently accurate for analyses of hydroextraction and filtration data. To avoid evaluating the integrals in these equations, when assessing sloping face hydroextractor cakes, the standard flow equation for a vertical face cake can be used with inner radius equal to the mean for the sloping face. The permeability estimated therefrom will be higher than the true value by a constant fraction dependent on face slope.

NOMENCLATURE

a, a' = constants cm
b = dimensionless constant.
g = gravitational acceleration cm/sec.^{2}
H = hydrostatic head in filtration tests ; cm
K = permeability (g/sec.^{2}) ; K_F for filtration; K_e for hydro-extraction.
L = cake thickness cm
n = speed of revolution rev. per sec.
n' = speed of revolution revs. per min.
p = pressure at position (x, y) inside cakes g/cm. sec.^{2}
q = rate of drainage through cakes ; q' from relaxation solutions, q'' from approximate equations cm^3/sec.
r = radius from axis of basket ; r_0 for cake outer surface ; r_e mean for cake inner surface ; r_L for liquid inner sur-surface ; r_w for basket inner surface cm
u = velocity in the direction of the x co-ordinate cm/sec.
v = velocity in the direction of the y co-ordinate cm/sec.
X = depth of the hydroextractor basket or width of wedge cakes cm
x = co-ordinate perpendicular to force field direction.
y = co-ordinate in the direction of the force field.
y' = difference between y ordinates of position on cake surface and cake surface at B in Fig. 2 where $x = X$.
μ = viscosity of liquid poise.
ω = angular velocity radians/sec.
ρ = density of liquid g/cm^3.
ϕ = velocity potential as defined by equation (6) ; ϕ' as defined by equation (11) cm^2/sec

REFERENCES

[1] BURAK, N. and STORROW, J. A.; J. Soc. Chem. Ind. 1950 69 8. [2] GUPTA, O. P.; M. Sc. Tech. thesis, Manchester 1948. [3] HARUNI, M. M. and STORROW, J. A.; Hydroextraction I Ind. Eng. Chem. 1952 44 2751. [4] HARUNI, M. M. and STORROW, J. A.; Hydroextraction II ibid. 1952 44 2756. [5] HARUNI, M. M. and STORROW, J. A.; Hydroextraction III ibid. 1952 44 2765. [6] HARUNI, M. M. and STORROW, J. A.; Hydroextraction IV, Chem. Eng. Sci. 1952 1 154. [7] HARUNI, M. M. and STORROW, J. A.; Hydroextraction V, Chem. Eng. Sci. 1953 2. 108. [8] INGLESENT, H. and STORROW, J. A.; Ind. Chem. 1951 27 76.

Frequency response analysis of continuous flow systems

H. KRAMERS and G. ALBERDA

Laboratorium voor Physische Technologie, Technological University, Delft, Netherlands

Summary—The distribution of residence times in a continuous flow system can de deduced from experiments concerning the behaviour of longitudinal concentration gradients on their course through the system. In this paper the application of sinusoidally varying concentrations is treated from a theoretical and experimental viewpoint. As an illustration of this frequency response analysis, experimental results are given for longitudinal diffusion in liquid flow through packed Raschig rings and for back-mixing of a liquid flowing over the packing of an absorption column.

Résumé—La répartition des " durées de séjour " de l'écoulement dans les systèmes en continu peut être déduit de la façon, dont un gradient longitudinal de la concentration se propage à travers le système. Ici on traite l'application des variations sinusoidales de la concentration, du point de vue théorique et experimentale. On présente des résultats expérimentaux de cette analyse harmonique: la diffusion longitudinale dans un liquide qui traverse un lit fixe d'anneaux Raschig et le mélange longitudinal d'un liquide descendant dans une colonne d'absorption à garnissage.

1. INTRODUCTION

The main purpose of this paper is to direct attention towards the possibilities of frequency response analysis of continuous processes in chemical engineering. We will mainly deal here with only one aspect of a continuous process, viz. the distribution of residence times in continuous flow systems. In this respect this paper can be regarded as a counterpart of a recent publication by DANCKWERTS [1], to which we shall frequently refer.

DANCKWERTS has given a general discussion on the distribution of residence times, which can be found by investigating the mode of propagation of an initial disturbance through the system. The distribution effect is best visualized if one suddenly changes a property (e.g. concentration) of the incoming stream from one steady value to another. The value of this property in the outflow as a function of time gives the response curve of the system to this initial step-wise disturbance. Such a response curve corresponds with the F-diagram in DANCKWERTS' paper. If the residence time is equal for all elements of the fluid entering the system, the response curve is again exactly a step function which is delayed with respect to the original disturbance by the time of residence. On the other hand if there is complete mixing in the system, the response curve to a step-wise disturbance is an exponential function. In between these two extreme types of F-diagrams one can find nearly all the response curves observed in practice. Their shape can be attributed to a number of phenomena for which various expressions are in use : longitudinal or axial diffusion, back-diffusion, back-mixing, short-circuiting, by-passing, channelling, trapping in dead corners, non-perfect mixing.

The aim of introducing a step-wise disturbance at the inlet of the continuous flow system is to obtain information regarding the actual distribution of residence times. Generally speaking, the same information can be obtained by analysing the response curve resulting from any kind of initial disturbance. As special cases the step-wise disturbance and also the delta-function (instantaneous injection) are convenient because their relation to the distribution function of the residence times is apparent. On the other hand they have two disadvantages. First, it is difficult to produce a sharp step – or delta-function in the concentration of a flowing liquid or gas exactly at the entrance of the system under investigation. With increasing demand for accurate results and with decreasing variation in residence times, the introduction of a signal of sufficient discontinuity in a stream becomes

impossible. In the second place, one encounters mathematical complexities when trying to calculate the response curves on the basis of an assumed physical mechanism. These are inherent in the non-stationary behaviour of the system under investigation.

The above difficulties can be partly overcome by applying a sinusoidal disturbance to the incoming stream. The measurement of the amplitude attenuation and the phase shift between the signals at the outlet and the entrance, as a function of the frequency of the signal, give complete information on the distribution of residence times of a system. The frequency response diagram thus obtained can eventually be transformed into a distribution curve by one of the practical methods of Fourier synthesis [2]. The main advantages of this harmonic analysis are that no discontinuities have to be introduced into the fluid streams, and that a steady cycling condition can be obtained. Furthermore the stationary operation simplifies the mathematical treatment of a few special problems, such as the case of a number of mixers in cascade or that of piston flow with longitudinal diffusion. Application of theory is restricted to so-called linear systems, where the dynamic behaviour is independent of the amplitude of the entering signal. As long as this signal does not interfere with the flow phenomena in the system this condition is satisfied. From the experimental point of view the frequency response method requires more elaborate equipment than the measurement of a response to a step- or delta-function.

The characterization of the dynamic behaviour of linear systems by the frequency response method is very well known in the field of servomechanisms and automatic control. The dynamic behaviour of a complete process involving, e.g. chemical reaction, transfer of heat or mass transfer can be investigated by the same technique with a view to the possible applications of automatic control. Profos [3] and Takahashi [4] have published such experiments on heat exchangers. A more general review of these problems has been presented by Rutherford [5] and by Aikman [6]. Frequency response measurements may also give information regarding the rate coefficients of heat or mass transfer in physical operations. Very recently, Wilhelm and Deisler [7], [8] have reported the first results of frequency response analysis applied to the inter- and intra-particle diffusion in gas flow through a fixed bed of porous catalyst carrier.

In the present paper we shall restrict ourselves to the purely hydrodynamical problem of the distribution of residence times. Firstly a brief survey will be given of the theoretical solutions for a few simple types of flow systems. Secondly some experimental viewpoints will be discussed together with illustrative results on longitudinal diffusion in liquid flow through Raschig rings and on the back-mixing of liquid flowing down a packed absorption column.

In the following we shall denote the deviation of the sinusoidal signal (e.g. tracer concentration) from its average value by c. For purposes of calculations it is customary to regard the signal as a complex harmonic function with a circular frequency ω. We then have for the value of the signal at any place in the system :

$$c = X\, e^{i\omega t}. \qquad (1)$$

X is a complex magnitude which can be represented by a radius vector in the complex plane, having a certain length (modulus) and phase angle (argument) with respect to the positive real axis. In the frequency response analysis the relationship between two signals c or their vectors X is of interest. It can be expressed by the ratio of their respective moduli (α) and the difference (ϕ) between their respective arguments. If we take for the two signals the concentrations of the effluent (c_e) of the system and of the incoming stream (c_i), the complex ratio between X_e and X_i is called the harmonic response function of the entire system. This function depends on the frequency ω of the applied signal in a way which is characteristic of the system. It contains both the amplitude ratio ($|X_e/X_i| = \alpha$) and the phase shift ϕ of X_e with respect to X_i and may be expressed as follows :

$$\frac{X_e}{X_i} = \alpha e^{i\phi}. \qquad (2)$$

In flow systems the outgoing signal is always smaller in amplitude and retarded in phase with respect to the entering signal, so generally $\alpha \leqslant 1$ and $\phi \leqslant 0$. A graphical representation of α and ϕ as a function of the frequency ω is called a frequency response diagram. Such a diagram can be obtained by measuring the amplitude ratio and the phase shift between an outgoing and incoming sinusoidal signal; for a number of special cases the harmonic response function can be calculated in a rather simple manner.

2. PERFECT MIXERS

By definition the concentration in a perfect mixer has a value at every point equal to the concentration at the outlet c_e. For continuous flow through the mixer we have the material balance:

$$c_i = c_e + \tau \frac{dc_e}{dt}, \tag{3}$$

where $\bar{\tau}$ is the average time of residence : volume of the mixer divided by the constant volumetric flow rate. If c_i is varied sinusoidally, we fined for the steady state after substitution of (1):

$$X_i = X_e + i\,\omega\bar{\tau}\,X_e, \tag{4}$$

and for the harmonic response function of one perfect mixer :

$$\frac{X_e}{X_i} = \frac{1}{1 + i\omega\bar{\tau}}. \tag{5}$$

The values of α and ϕ are found to be :

$$\left.\begin{array}{l} \alpha_1 = (1 + \omega^2\,\bar{\tau}^2)^{-\frac{1}{2}} \\[2mm] \phi_1 = -\tan^{-1}\omega\bar{\tau}. \end{array}\right\} \tag{6}$$

Applying the result (5) to a system containing n perfect mixers in cascade having equal times of residence $\bar{\tau}/n$, we get for the response function between X_e and X_i :

$$\frac{X_e}{X_i} = \left(1 + i\omega\frac{\bar{\tau}}{n}\right)^{-n} \tag{7}$$

with the following values of α and ϕ :

$$\left.\begin{array}{l} \alpha_n = \left(1 + \dfrac{\omega^2\,\bar{\tau}^2}{n^2}\right)^{-n/2} \\[4mm] \phi_n = -n\tan^{-1}\dfrac{\omega\bar{\tau}}{n}. \end{array}\right\} \tag{8}$$

Fig. 1 gives the frequency response diagrams for systems containing different numbers of
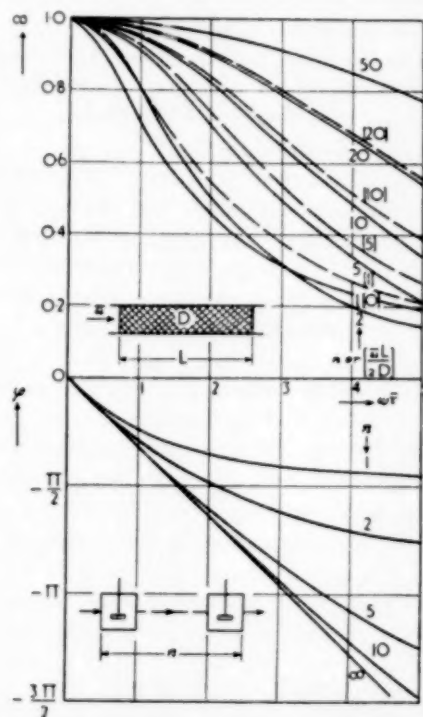

Fig. 1. Frequency response diagram for n equal mixers in cascade (———) and for piston flow with longitudinal diffusion (— — —).

mixers in series with a total average residence time $\bar{\tau}$.

A special case of (7) presents itself for $n \to \infty$:

$$\operatorname*{Lim}_{n\,\to\,\infty}\left(1 + i\omega\frac{\bar{\tau}}{n}\right)^{-n} = e^{-i\omega\bar{\tau}}, \tag{9}$$

so that here :
$$\left.\begin{array}{l} \alpha_\infty = 1 \\[3mm] \phi_\infty = -\omega\,.\bar{\tau} \end{array}\right\} \tag{10}$$

This case is represented by perfect piston flow where no amplitude attenuation of the incoming

signal occurs and where the phase lag is caused by the pure distance-velocity lag. There is no mixing or diffusion in the direction of flow.

The frequency response diagram of a real system generally lies in between those for one perfect mixer and for perfect piston flow. However, it is not at all necessary that the diagram for a real system coincides with one for a certain number of perfect mixers.

It is to be noted the equations (5), (7) and (9) have the same form as those for the fractional completion of a first order chemical reaction in continuous flow through well agitated vessels. The relation between the reactant concentrations leaving and entering one perfect mixer is in that case represented by eq. (4) if the operator $i\omega$ is replaced by the first order reaction velocity constant. Chemical reactions in continuous stirred tank systems have been amply discussed by McMullin and Weber (9), Eldridge and Piret (10) and Schoenemann (11). The harmonic response function of any system of stirred tanks, with or without external recirculation can be calculated with the same relative ease as the yield of a first order chemical reaction in these systems. The extraction of the amplitude and phase relationships from the complex response function presents no difficulties, although in some cases it may involve elaborate computational work.

3. Piston Flow with Longitudinal Diffusion

In a number of systems the distribution of residence times can be regarded as the combined result of perfect piston flow and a coefficient of longitudinal diffusion D. Generally the role of molecular diffusion is rather unimportant. In flow through fixed beds of solids and in beds in which particulate fluidization occurs the small-scale fluctuations of the intergranular fluid velocity cause a statistical distribution of residence times which can be interpreted as the result of an " eddy " diffusivity. The same applies to a tubular reactor in which a uniform degree of turbulence is created by mechanical means. The introduction of a longitudinal diffusivity has significance only if the underlying phenomenon is of a statistical nature, i.e. if the

elementary fluctuations are repeated many times during the course of the fluid through the system. Marcrophenomena, such as by-passing and trapping, make the picture of diffusion inadequate.

The differential equation for the concentration in a system (Fig. 2) with uniform flow velocity
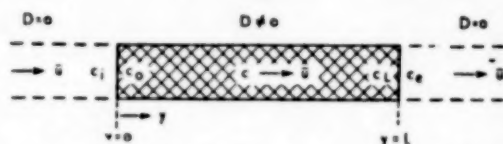

Fig. 2. Packed tube with piston flow and longitudinal diffusion.

u and a longitudinal diffusivity D is :

$$\frac{\partial^2 c}{\partial y^2} - \frac{\bar{u}}{D}\frac{\partial c}{\partial y} - \frac{1}{D}\frac{\partial c}{\partial t} = 0 . \qquad (11)$$

It is now assumed that the system has a finite length L and that a constant diffusivity D exists over the cross-sectional area and for $0 \leqslant y \leqslant L$. For $y < 0$ and $y > L$, $D = 0$. This leads to the following boundary conditions :

$$\bar{u}c_i = \bar{u}c - D\frac{\partial c}{\partial y}, y = 0 \qquad (12)$$

and

$$\bar{u}c_e = \bar{u}c - D\frac{\partial c}{\partial y}, y = L. \qquad (13)$$

The latter condition has to be supplemented by the condition $c_e = c_L$, which appears to be necessitated by the physical conditions at the exit. Therefore (13) has to be replaced by :

$$\frac{\partial c}{\partial y} = 0 , y = L . \qquad (14)$$

In order to solve eq. (11) for a sinusoidally varying input signal c_i and for steady conditions we introduce the substitution given by eq. (1). The partial differential equation (11) then reduces to the following ordinary linear differential equation with constant coefficients :

$$\frac{d^2 X}{dy^2} - \frac{\bar{u}}{D}\frac{dX}{dy} - \frac{i\omega}{D}X = 0 , \qquad (15)$$

with the boundary conditions :

$$X_i = X - \frac{D}{\bar{u}}\frac{dX}{dy} , \quad y = 0$$
$$\frac{dX}{dy} = 0 \qquad , \quad y = L . \qquad (16)$$

These equations are identical with those given by DANCKWERTS ([1], eq. (30), (31) and (32)) for the reactant concentration resulting from a first order chemical reaction in a similar flow system. The harmonic response function X/X_i can be deduced directly from DANCKWERTS' general solution (eq. (33)) if the reaction velocity constant k is replaced by $i\omega$. For the reponse function of the entire system we have :

$$\frac{X_e}{X_i} = \frac{4p}{(1+p)^2\exp\dfrac{-\bar{u}L}{2D}(1-p)-(1-p)^2\exp\dfrac{-\bar{u}L}{2D}(1+p)} , \qquad (17)$$

where $p = \sqrt{1 + 4\,i\omega\,D/\bar{u}^2}$.

This function depends on two variables for which we choose the dimensionless groups $\omega L/\bar{u} = \omega\bar{\tau}$ and $2D/\bar{u}L$. The latter number can be regarded as the ratio between the average time of residence $L/\bar{u} = \bar{\tau}$ and the diffusion time constant for the length $L :$ $\tau_D = L^2/2D$. For $\bar{\tau}/\tau_D = 2D/\bar{u}L > 1$, all concentration differences are levelled out relatively rapidly by diffusion. For the limiting of $D = \infty$, we find that eq. (17) is indentical with the response function for one perfect mixer, eq. (5). As $\bar{\tau}/\tau_D$ decreases, the influence of diffusion becomes less important, In the limiting case $\bar{\tau}/\tau_D = 2D/\bar{u}L = 0$ eq. (17) yields the solution for perfect piston flow, eq. (9).

For small values of $2D/\bar{u}L$, eq. (17) can be approximated by

$$\frac{X_e}{X_i} \cong \left(1 - \frac{\omega^2 DL}{\bar{u}^3}\right)e^{-i\omega L/\bar{u}} , \quad \frac{\omega D}{\bar{u}^2} < 1 , \quad (18)$$

giving

$$\ln\frac{X_e}{X_i} \cong - i\,\frac{\omega L}{\bar{u}} - \frac{\omega^2 DL}{\bar{u}^3} + \dots \qquad (19)$$

At the same time eq. (5) for n equal mixers may be approximated for large values of n by :

$$\ln\frac{X_e}{X_i} \cong - i\omega\bar{\tau} - \frac{\omega^2\bar{\tau}^2}{2n} + i\,\frac{\omega^3\bar{\tau}^3}{3n^2} + \dots \qquad (20)$$

Comparison of (19) and (20) shows that perfect piston flow with longitudinal diffusion yields the same frequency response diagram as a number of n perfect mixers with the same total residence time $\bar{\tau}$, if

$$\frac{1}{n} \cong \frac{2D}{\bar{u}L} , \quad \frac{\omega\bar{\tau}}{n} < 1 .^* \qquad (21)$$

The physical interpretation of this equation is as follows. Suppose we divide the reactor of Fig. 2 into n parts of equal length L/n. For this length the average time of residence is $L/n\bar{u}$ and the diffusion time constant is $L^2/2Dn^2$. Apparently, when the relation (21) holds, both times are equal.

The validity of equation (21) is restricted to very high values of n or of $\bar{u}L/2D$. The diagram of Fig. 1 shows the amplitude curves for various values of $\bar{u}L/2D$. Comparing these with the curves for perfect mixers one is inclined to accept the more general connection between n and D :

$$\frac{1}{n-1} \cong \frac{2D}{\bar{u}L} . \qquad (22)$$

This analogy may be used for n greater than 5 to 10, depending on the accuracy required. It also holds for $n = 1$, but is a quite insufficient approximation in the intermediate region. The phase lags of two systems which are analogous in the sense of eq. (22) are not materially different for $\omega\bar{\tau} < 5$, mainly because in this region the phase lag is rather insensitive to changes in n or $D/\bar{u}L$. The practical advantage of the analogy (22) is that for flow systems have a relatively small diffusivity the frequency response diagrams can be calculated from eq. (8) which is more convenient in handling than eq. (17).

4. POISEUILLE FLOW

The harmonic response function for laminar flow in a tube with a circular cross-section is

---

* By personal communication, we were informed that DR. G. H. REMAN (Royal Dutch/Shell Laboratory, Amsterdam) arrived at the same analogy by comparing the step-function response functions of the two types of system.

illustrative of cases where the flow rate is non-uniform. In the following we assume that there is neither radial nor axial diffusion and that the velocity distribution is given by
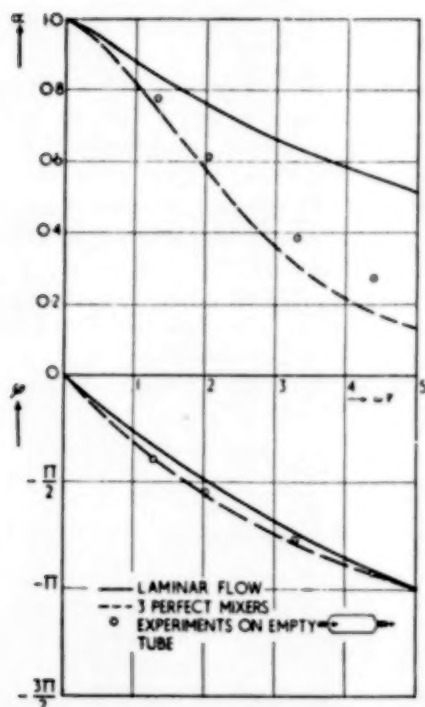
$$u = 2\bar{u}\left(1 - \frac{r^2}{R^2}\right). \tag{23}$$

Fig. 3. Frequency response diagram for Poiseuille flow in a tube (————) as compared with that of 3 equal mixers in series (— — —).

The time of residence for a streamline at a distance r from the axis is u/L. As there is no backmixing in the streamline its response function represents a pure distance-velocity lag, $\exp -i\omega L/u$ according to (9). Integrating for all streamlines multiplied by their velocities one finds for the harmonic response function between the average outlet signal and the incoming signal :

$$\frac{X_e}{X_i} = \frac{1}{\pi\bar{u}R^2}\int\limits_0^R e^{-i\omega L/u} u\, 2\pi r\, dr\,. \tag{24}$$

The frequency response diagram calculated from (24) has been drawn in Fig. 3. It shows less phase lag and more amplitude damping than piston flow. Its phase behaviour might be compared with that of 3 perfect mixers in series, at least for $\omega\bar{\tau} < 5$. The amplitude attenuation however is much less than for 3 mixers. This feature is indicative of a non-uniform velocity distribution which also may be caused by channelling and trapping.

5. REMARKS ON THE EXPERIMENTAL TECHNIQUE

For frequency response measurements on a continuous flow system one needs first of all a good property to use as a " signal " and a means of measuring it. In the second place a mechanism for introducing the signal sinusoidally is required.

For measuring the distribution of residence times the concentration of any material which is miscible with the main flow and does not disappear by reaction, adsorption or desorption, can be used as a " signal." Considerable variations in concentration may cause undesirable convection currents as a result of densitygradients. The choice of the tracer component is further restricted by the requirements of the concentration measurement : a quick response with respect to the lags of the system, continuous measurement or recording, a high degree of accuracy and linearity. For liquid flow the most convenient " signal " is the concentration of an appropriate electrolyte in water, which can be measured by the electric conductivity. In the case of gas flow, currently available devices for measuring gas composition have a response which is too slow to be used for this kind of investigation. Only the gas analyser described by DEISLER and WILHELM [8], [12] seems to meet the special requirements in all respects. With this instrument one measures the ionization current in a gas which is exposed to alpha-radiation from a radio-active source. It indicates concentrations linearly and has a time lag of the order of one second. Although for liquids and gases radioactive tracers could be used, this method appears to be very costly if continuous indication or recording of the concentration is required.

There are many possible devices for producing

a constant flow with a sinusoidally varying concentration. Generally it amounts to the addition of a concentrated solution or mixture to the main stream, at a relatively small rate which is varied periodically with different frequencies. This flow can be given the desired fluctuation by simply turning an appropiate valve, by mechanically varying the discharge of a feeder pump or by using a constant discharge pump combined with a sinusoidally varying buffer volume. A more costly way of regulating the additional flow incorporates an automatic controller the setpoint of which is varied in a sinusoidal way.

For quantitative measurements it is important that the entering signal contains no higher harmonics. The latter are damped relatively quickly so that too small an amplitude ratio α may be found. In the experiments to be reported in the next section, we used a variable stroke pump for feeding the concentrated solution. The signal obtained after mixing with the main stream contained higher harmonics due to the reciprocating action of the pump and to some backlash in the mechanism for varying the stroke. These harmonics were filtered off in a packed column of suitable length in the same way as has been reported by Deisler and Wilhelm [8].

6. Experimental Results

The results of some preliminary measurements will be discussed here in order to illustrate the preceeding sections and to show the feasibility and the limitations of the frequency response technique.

Longitudinal mixing was investigated for flow of water through a tube (diameter 7·4 cm., length 34 cm.) with 10 mm Raschig rings (fractional free volume 0·75). Fig 4 shows the resulting frequency response diagram of X_e/X_i for the two water velocities investigated (1·2 and 2·2 cm/sec). In the amplitude diagram the experimental points lie in between the curves for $\bar{u}L/2D = 15$ and 20. The points in the phase diagram suggest a smaller value of the order of 10, the discrepancy probably being caused by a certain amount of trapping in the interior of the rings. As the amplitude curve is the more

accurate one, we have deduced from these measurements that for both flow velocities

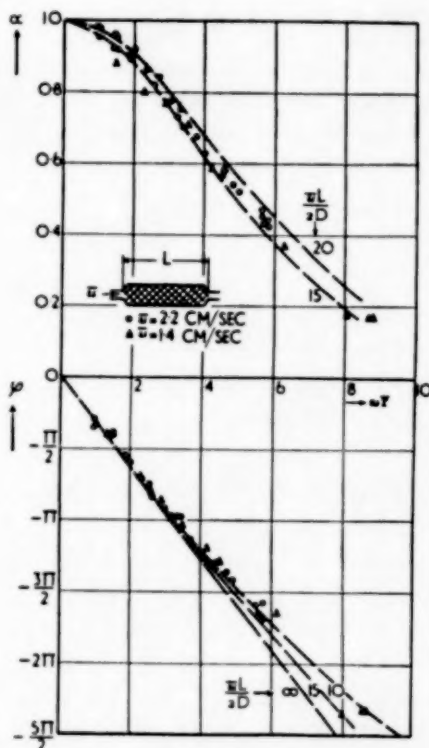$$\frac{\bar{u}L}{2D} \cong 15 .$$

Fig. 4. Frequency response measurements of liquid flow through a packed tube (Raschig rings 10mm).

Relating D to the nominal ring diameter d_r, we have

$$\frac{D}{\bar{u}d_r} = \frac{D}{\bar{u}L} \times \frac{L}{d_r} = 1\cdot1 \pm 0\cdot1 ; \; 100 < \frac{\bar{u}d_r}{\nu} < 200 .^*$$

The observed longitudinal diffusivities are about 10 times greater than those reported by Wilhelm [7] for radial diffusion with liquid flow through a bed of packed spheres. As with radial diffusion, a proportionality between D and $\bar{u}$ seems to exist in the flow region covered.

---

* Danckwerts [1] found from the response curve to a step-wise disturbance of a similar system with about the same packing and $\bar{u} = 0\cdot4$ cm/sec : $D/\bar{u}d_r = 1\cdot8$.

179

Frequency response measurements for water flow in the same tube (diameter 7·4 cm, length 34 cm and $\bar{u} = 2·1$ cm/sec) without any packing yielded the results which have been plotted in Fig. 3. Although under these conditions laminar flow would be realized in a sufficiently long tube, here the turbulence created by the sudden enlargement at the liquid inlet causes the system to behave in about the same manner as three equal mixers in series, which is purely accidental.
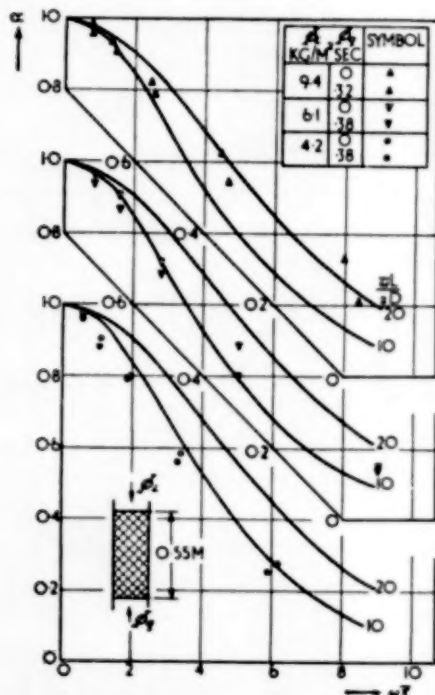

Fig. 5. Amplitude-frequency characteristics of liquid flow over the packing of an absorption column with and without counter-current gas flow.

Finally, we mention a number of experiments on the distribution of residence times of water running over the packing in an absorption column with a countercurrent air flow. These measurements were carried out in a 15 cm diameter column with a 66 cm high packing of 10 mm Raschig rings. The water feed was uniformly distributed over the top of the packing. The outgoing liquid was separated from the gas and

mixed with the shortest possible lag before its concentration was recorded. The average residence time, which depends on the liquid hold-up of the system, was determined from the measured phase shifts for small $\omega\bar{\tau}$ values. In this region ϕ should be equal to $-\omega\bar{\tau}$ in view of the rather small amount of back-mixing. Experimental runs were made at three liquid flow rates ϕ_L, both without and with air flow ϕ_G which was adjusted somewhat below the flooding rate.

The experimental results have been plotted in Fig. 5 for the amplitude diagram only, together with the theoretical curves for $\bar{u}L/2D = 10$ and 20. Evidently the results cannot be ascribed to the presence of longitudinal diffusivity only. Presumably this is due to the non-uniform velocity distribution which is well known to occur in packed absorbers as a consequence of preferential wetting near the wall. On the other hand the results clearly show that back mixing of the liquid is increased with decreasing liquid load and increasing gas load. The latter effect was, of course, to be expected, but it appears that under normal operating conditions it would not seriously impair the separating efficiency of an absorber.

ACKNOWLEDGMENT

REFERENCES

[1] DANCKWERTS, P. V.; Chem. Eng. Sci. 1953 2 1. [2] HAMOS, L. VON, JANSSON, B., PERSSON, Th.; Acta Polytechnica 1952 112, Physics and Applied Mathematics Series vol. 2, nr. 3. [3] Profos, P.; Vektorielle Regeltheorie, Diss. Zürich, 1943. [4] TAKAHASHI, Y.; Regelungstechnik 1953 1 32. [5] RUTHERFORD, C. I.; Proc. Inst. Mech. Engrs. (London) 1950 162 334. [6] AIKMAN, A. R.; Regelungstechnik 1953 1 4. [7] WILHELM, R. H.; Chem. Eng. Progress 1953 49 150. [8] DEISLER, P. F., WILHELM, R. H.; Ind. Eng. Chem. 1953 45 1219. [9] McMULLIN, R. B., WEBER, M.; Trans. Am. Inst. Chem. Engrs. 1935 31 409. [10] ELDRIDGE, J. W., PIRET, E. L.; Chem. Eng. Progress 1950 46 290. [11] SCHOENEMANN, K.; Dechema Monographs 1952 21 203. [12] DEISLER, P. F.; Diss. Princeton University, 1952, Part II.

NOTATION

c = deviation of concentration from average value ; c_i entering the system ; c_e leaving the system

d_r = nominal diameter of Raschig rings

D = apparent longitudinal diffusivity

L = length of tube or column

n = number of equal mixers in series

r = variable distance from tube axis

R = radius of tube

t = time

u = flow velocity ; $\bar{u}$ average (intergranular) velocity

X = symbol representing concentration vector in the complex plane

y = length coordinate in the direction of flow

α = amplitude ratio between outgoing and incoming concentration c

ν = kinematic viscosity

$\bar{\tau}$ = average time of residence in the system

ϕ = phase shift between outgoing and incoming concentration c (radians)

ω = circular frequency (rad/sec)

Production of phenol from cumene

J. P. Fortuin* and H. I. Waterman

Laboratory of Chemical Engineering, The University, Delft, Holland

Summary—This paper deals with the preparation of phenol from cumene. Liquid-phase oxidation of cumene with molecular oxygen produces cumene hydroperoxide, which is subsequently decomposed catalytically into phenol and acetone.

The oxidation requires the use of thoroughly purified cumene. It was carried out in a copper vessel at 120°C, good conversions and high yields of cumene hydroperoxide being obtained.

For the decomposition of cumene hydroperoxide into phenol and acetone sulphur dioxide was used as the catalyst. This reaction gave optimum results when carried out in a film reactor.

A description is given of an apparatus for continuous preparation of phenol from cumene and a simplified flow sheet for production on a larger scale is added.

Résumé—L'auteur étudie la préparation de phénol à partir de cumène. L'oxydation en phase liquide du cumène par l'oxygène moléculaire donne l'hydroperoxyde de cumène qui est ensuite décomposé par voie catalytique en phénol et en acétone.

L'oxydation demande l'emploi de cumène de haute pureté. Effectuée dans un récipient en cuivre à 120°C elle donne de bonnes transformations et de hauts rendements en hydroperoxyde de cumène.

Pour la décomposition en phénol et en acétone de l'hydroperoxyde ainsi obtenu l'auteur utilise l'anhydride sulfureux SO_2 comme catalyseur. On obtient les meilleurs résultats lorsque la décomposition est exécutée dans un réacteur où le liquide est décomposé sous forme d'une couche mince.

L'auteur décrit un appareil pour la préparation continue de phénol à partir de cumène et un schéma simplifié d'opération pour la production à plus grande échelle.

Introduction

Recently a new process for commercial phenol production has been announced, with cumene (isopropylbenzene) as starting material [1]. The process is obviously based upon the reactions first disclosed by Hock and Lang [2].

cumene · cumene hydroperoxide · phenol · acetone
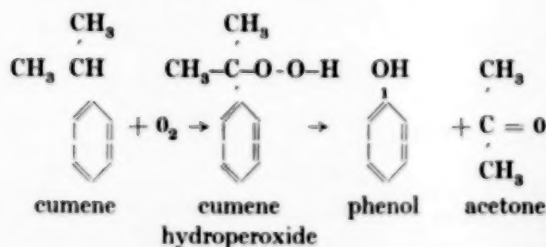
The further development of this new phenol synthesis necessitated a laboratory investigation into both reactions. The present paper discusses the main features of this work. During the investigation several patents and applications were published by others interested in the field.

Preparation of Cumene Hydroperoxide

Hock and Lang prepared cumene hydroperoxide by bubbling dry oxygen through cumene heated at 85°C under ultra-violet radiation [2]. Only $7\frac{1}{2}$ per cent of the cumene had been converted to the hydroperoxide after 24 hours.

Oxidation of a cumene-water emulsion system gave conversions to cumene hydroperoxide of 30-40 per cent and yields of 80-90 per cent [3]. About 3 per cent wt of cumene hydroperoxide was formed per hour in the hydrocarbon layer. Still better reaction rates were obtained when the cumene was oxidized as such at 110-130°C [4]. At 120°C 7 per cent wt of cumene hydroperoxide was formed in the liquid per hour.

Previous addition of cumene hydroperoxide to the cumene to be oxidized is claimed to shorten the induction period and thus to increase the reaction rate [5].

As catalysts $CaCO_3$, Na_2CO_3 [6] or lead salts [7] are mentioned. Even with the aid of these catalysts the reaction rates remained low (about

* Present address : *Koninklijke/Shell-Laboratorium Amsterdam* Holland.

1-3 per cent wt of cumene hydroperoxide formed per hour).

It may be concluded that the oxidation rates generally are very low. The yield of cumene converted into cumene hydroperoxide may be as high as 90-100 per cent, however. One of the objects of the investigation was therefore to increase the reaction rate whilst maintaining a high yield, so as to develop an oxidation process attractive for the manufacture of cumene hydroperoxide on a larger scale.

Technical cumene from several sources was used as the starting material.

ANALYTICAL PROCEDURE

All hydroperoxide concentrations were determined by an iodometric method [8]. This method

Table 1.

Accuracy of the analysis of cumene hydroperoxide

Concentration of cumene hydroperoxide % wt	Found by analysis % wt		Mean	Deviation
20·0	19·5	19·6	19·6	− 0·4
50·0	48·1	48·2	48·2	− 1·8
100·0	95·8	95·7	95·8	− 4·2

was checked with pure cumene hydroperoxide (prepared from the recrystallized sodium salt, cf. HOCK and LANG [2]) and with solutions of cumene hydroperoxide in cumene of known strength. The results are summarized in Table 1.

Duplicate determinations were reproducible within 0·1 per cent. The table shows that the results are somewhat too low. The deviation increases with increasing cumene hydroperoxide content. No correction was made for this deviation in the experimental work.

APPARATUS

The first oxidation experiments were carried out in a pyrex reactor (capacity approx. 400 ml, see Fig. 1). The dispersion of the oxygen in the liquid was effected with a nozzle and a stirrer.

The oxygen was of commercial quality containing at least 99 per cent O_2. When air was used as the oxidant it was first filtered through cotton wool.

PURITY OF THE FEED

Technical cumene absorbed only a very small amount of oxygen at 120°C in the pyrex reactor. No hydroperoxide could be detected in the reaction mixture.

Rectification of the technical products yielded a cumene fraction, boiling range 152·0-152·5°C, n_D^{20} 1·4913 (lit.b.p. 152·3°C, n_D^{20} 1·4913 [9]). This fraction, however, still refused to absorb an appreciable amount of oxygen at 120°C within six hours. It was suspected that the cumene contained inhibitors which had not been removed by distillation.

Chemical treatments to improve the oxidizability of cumene are described in the literature, i.e. boiling with sodium [2], washing with bisulphite or permanganate solutions [5] or with sodium hydroxide [6].

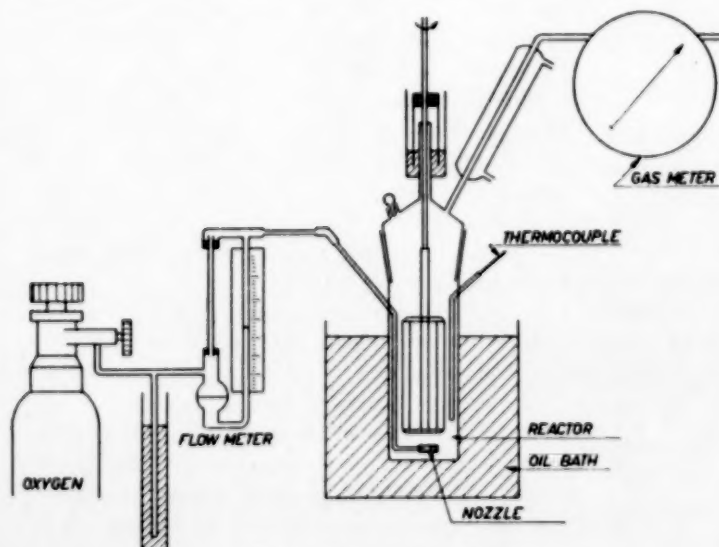Several methods have been tested. For this purpose the crude cumene was first distilled,

Fig. 1. The pyrex reactor.

the fraction boiling between 151-156°C being sub-
jected to several treatments. The treated cumene
was then dried over calcium chloride, distilled
again and the fraction with n_D^{20} 1·4913 oxidized
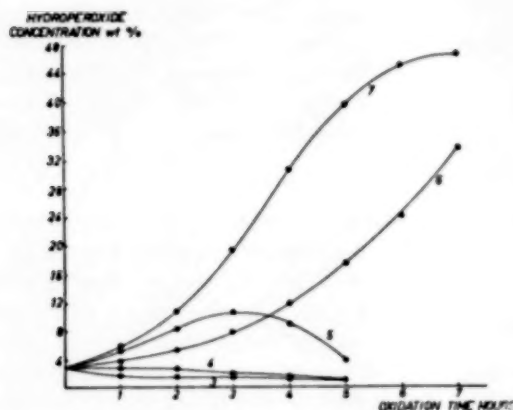in the pyrex reactor.

Fig. 2.   Purification of cumene.

Experimental

The following treatments were applied :

1. Permanganate treatment.

250 ml cumene was agitated for 10 mins with
200 ml 3 per cent aqueous $KMnO_4$ solution, then
washed with 2 n caustic soda solution and with
water.

2. Bisulphite treatment.

250 ml was twice agitated for 10 mins with 100 ml
of a 5 per cent aqueous solution of sodium bisul-
phite solution, then washed with water.

3. Hypochlorite treatment [10].

500 ml cumene was agitated for 15 mins with
80 ml 6 n acetic acid and 300 ml of an aqueous
hypochlorite solution which contained 22·5 grams
of bleaching powder, comprising 27·4 per cent wt
of active chlorine.   After separation the treated
cumene layer was washed with water.

4. Sodium hydroxide treatment.

500 ml cumene was twice agitated for 10 mins
with 20 ml of a 25 per cent aqueous solution of
NaOH and then twice with 100 ml water.

5. Sodium treatment.

500 ml cumene was boiled for 1 hour with 15
grams of sodium.

6. Sulphuric acid treatment.

800 ml of cumene was thrice agitated for 10 mins
with 20 ml of sulphuric acid (96 per cent, spec. wt
1·84), then washed with water, 2 n sodium hydro-
xide solution and again with water.

7. Double sulphuric acid treatment.

800 ml of cumene was subjected to the same
treatment as described under 6 with the only
difference that the agitation with sulphuric acid
was repeated six times instead of three times.

Oxidation tests were carried out by bubbling
through oxygen gas at a rate of between 9 and
10 1/h.   In each run 200 ml of cumene was used
to which 3·0 per cent wt of cumene hydroperoxide
had been added as initiator.   The temperature
during the oxidation was 120°C.   The hydro-
peroxide content of the oxidized liquids was
determined at hourly intervals.   The results of
treatments 1 and 2 were entirely negative, no
cumene hydroperoxide being formed in the
liquids.   The results of the other tests are shown
in Fig. 2.

It is clear that the treatment with concentrated
sulphuric acid gave the most satisfactory results.
In some instances, however, a treatment with
sulphuric acid did not yet provide reproducible
oxidation rates.   It was found that in those cases
the oxidizability could be restored if a second
purification step was added.   After the double
sulphuric acid treatment the cumene was then
agitated twice for 5 mins with a 5 per cent aqueous
solution of mercuric acetate followed by a caustic
soda and a water wash.

Technical cumene is prepared by catalytic
alkylation of benzene with propylene.   Sulphuric
acid, phosphoric acid (on a carrier) or aluminium
chloride are generally used as catalysts.   Con-
tamination of the crude cumene with thiophenes,
propylene polymers or styrenes is therefore very
likely.   Which of the possible contaminants acted
as inhibitors was investigated by adding 1/4 mol
per cent of these substances to purified cumene
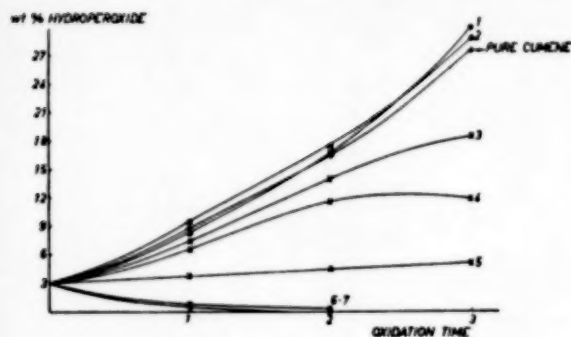and measuring the oxidation rate of the liquids
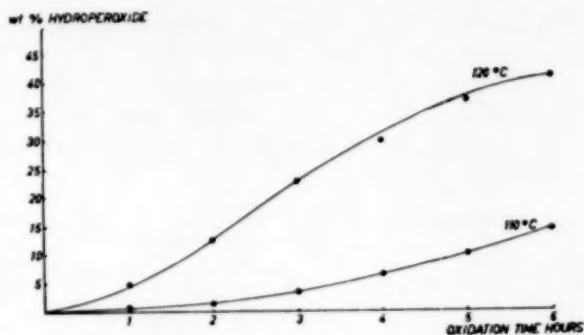
Fig. 3.   Inhibitors in cumene oxidation.

Fig. 4.   Liquid phase oxidation of cumene.

so obtained. These experiments were carried out in the pyrex reactor. The results are shown in Fig. 3.

Experimental

To 200 ml of purified cumene comprising 3 per cent wt of cumene hydroperoxide (as initiator) was added in each test 1/4 mol per cent of one of the following substances :

1. p. chlorotoluene	b.p. 161–163°C
2. nonene-3	b.p. 150·2–150·4°C
3. α-methyl styrene	b.p. 162–164°C
4. aniline	b.p. 182°C
5. phenol	m.p. 41°C
6. thiophenol	b.p. 166–169°C
7. isopropylthiophene [11]	b.p. 160–180°C

The oxidation was carried out at 120°C, 9 l of oxygen being passed through the liquid per hour. The hydroperoxide concentrations were determined at hourly intervals.

The results indicate that especially the sulphur compounds should be removed from the cumene. Contamination with phenol, aniline or α-methyl styrene should be avoided as well. It is clear that a suitable purification method for cumene depends upon the nature of the inhibitors present in the crude.

EXPERIMENTS IN THE PYREX REACTOR

It was shown that the oxidation rate of cumene depends strongly on the purity of the feed. Comparative experiments were therefore carried out with batches of the same liquid.

The experiments in the pyrex reactor were carried out with a stirrer speed of 1,200 r.p.m. No appreciable change in oxidation rate was observed when varying the stirrer speed between 1,000 and 1,400 r.p.m. Neither had the throughput of oxygen (if between 5 and 15 1/h) any effect on the oxidation rate.

The variation of the hydroperoxide concentration with time during the oxidation of batches of 200 ml of purified cumene at 110 and 120°C is shown in Fig. 4.

A long induction period is observed at 110°C. By previous addition of cumene hydroperoxide this induction period may be avoided, thus decreasing the total reaction time considerably.

The yield of the oxidation was computed from the hydroperoxide content and the total oxygen content of the liquids.

$$\text{Yield }\% = \frac{\substack{\% \text{ wt of oxygen bound as hydro-}\\ \text{peroxide in the liquid}}}{\% \text{ wt total oxygen in the liquid}} \times 100$$

Table 2

Yields of the oxidation experiments in the pyrex reactor

Temperature °C	Oxidation period h	% wt cumene hydroperoxide formed	% wt active oxygen	% wt total oxygen (100-%C -%H)	Yield %
110	6	13·6	2·86	3·17	90·2
120	6	40·6	8·55	10·14	84·3
130	5	35·8	7·54	10·10	74·6

The yield decreases rapidly as the temperature

185

is raised. 110°C seems the best reaction temperature in this apparatus.

Some experiments were carried out with air as the oxidant. Copper turnings or finely divided silver were added as catalysts. The results are given in Fig. 5.
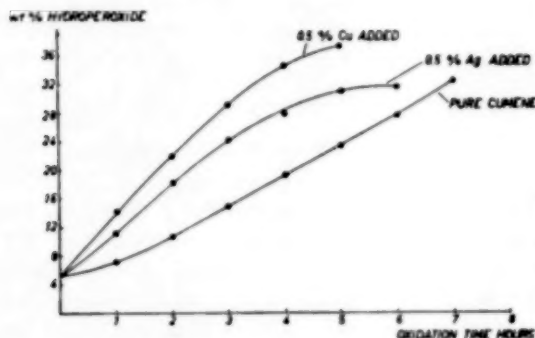

Fig. 5. Oxidation of cumene with air.

Experimental

Oxidation temperature 110°C; throughput of air 15 l/h. Stirrer speed 1,200 r.p.m. 200-ml batches of cumene to which 5·4 per cent wt of cumene hydroperoxide had been added as initiator.

About the same maximum oxidation rate is observed with air as with oxygen at 110°C, which indicates that the rate is independent of the oxygen concentration.

Under these conditions the hydroperoxide formation is catalysed by the metals.

EXPERIMENTS IN A COPPER REACTOR

Addition of copper bronze during the oxidation of cumene exerts a catalytic effect. It was found, moreover, that cumene hydroperoxide shows a marked stability in copper compared with glass or iron at 110°C [12]. Therefore, the preparation of cumene hydroperoxide was now studied using a copper vessel as the reactor. The reactor employed is shown in Fig. 6. The content of the vessel was approx. 350 ml.

Before each experiment the inner surface of the reactor was rinsed with fuming nitric acid (spec. gr. 1·52) then washed with water and dried.

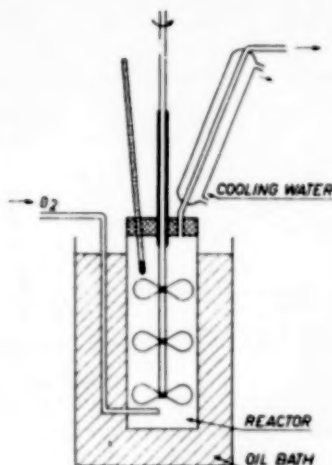No stirrer was applied in the first experiments. To increase the active surface area copper or

Fig. 6. The copper reactor.

silver on pumice were added. These catalysts were prepared by adsorption of the complex ammonia compounds of the metals on pumice, followed by reduction with hydrogen [13]. Batches of 250 ml of purified cumene were used in the experiments, which were carried out at 120°C with an oxidation period of 3 hours.

Table 3.

Experiments in the copper reactor (without stirrer).

Oxidant	l/h	Catalyst	Cumene hydroperoxide concentration	
			initial % wt	final % wt
air	50	5 g pumice	5·4	16·6
air	50	5 g Cu on ,,	5·4	16·6
air	50	5 g Ag on ,,	5·4	17·3
oxygen	25	5 g Ag on ,,	4·6	24·9

The addition of metallic catalysts is of no value here. It was noted, however, that with the silver catalyst added the resulting peroxide solution was nearly water-white, whilst the other oxidized liquids were uniformly yellow coloured.

As no stirring is applied the oxygen pressure influences the oxidation rate here, the rate-determining step being the diffusion of oxygen into the liquid.

In the next series of experiments a copper stirrer was used (as can be seen in Fig. 6, stirred speed 880 r.p.m.) 225 ml of purified cumene was oxidized in each run with oxygen, introduced at a rate of 25 1/h. No initiator was added, as it was observed that the oxidation in the copper reactor proceeded without an induction period. The results are given in Table 4.

Table 4

Experiments in the copper reactor

Temperature °C	Oxidation period h	Final hydroperoxide conc. % wt	Total oxygen in liquid % wt	Yield %
120	1	11·0	2·45	95
120	2	22·5	5·08	93
120	3	34·7	7·54	96
130	1	25·0	6·50	81
130	2	34·4	—	—

High yields were obtained at 120°C, which seems to be the best oxidation temperature in this apparatus. The reproducibility of these results was good. Generally 11-13 per cent wt of cumene hydroperoxide was formed per hour on oxidation at 120°C, when cumene of high purity was used. These rates are considerably higher than those mentioned in the literature for cumene oxidation.

DECOMPOSITION OF CUMENE HYDROPEROXIDE

HOCK and LANG heated cumene hydroperoxide with a large excess of 10 per cent sulphuric acid for 1½ hours at 100°C. A 75 per cent yield of phenol was obtained, the presence of acetone being qualitatively demonstrated [2].

This reaction was studied afterwards by KHARASCH and collaborators [14]. Under the catalytic influence of acids (as conceived by LEWIS) almost exclusively phenol and acetone were obtained from cumene hydroperoxide. According to these investigators the cleavage of the hydroperoxide proceeded as a chain reaction through an ionic mechanism.

The patent literature discloses the use of sulphuric acid [15], acidic condensation – or Friedel Crafts type catalysts [16] and sulphur or phosphorus [17].

In our investigation sulphur dioxide was used as the catalyst. High yields of phenol and acetone were obtained from the cumene hydroperoxide.

Later it appeared that a patent application had been filed for the use of sulphur dioxide as a catalyst in this reaction [18]. It was also mentioned by KHARASCH [14].

Experimental

When SO_2 gas is fed into a flask containing some grams of pure cumene hydroperoxide the liquid explodes almost immediately. The reaction proves to be strongly exothermic.

Even at very low temperatures sulphur dioxide is still active. When cumene hydroperoxide was added dropwise to liquid SO_2, which was kept at a temperature of − 55°C, there was again a heavy explosion after some time. We assume that the reaction set in after a given quantity of hydroperoxide had accumulated in the liquid sulphur dioxide and ended in an explosion as the result of insufficient heat removal.

Temperature control is of particular importance here, for the hydroperoxide will decompose to an increasing extent according to an alternative reaction when the temperature is raised. As is known, the main products formed during thermal decomposition are acetophenone and methyl alcohol. It is obvious therefore that, if during the catalytic decomposition the temperature is not sufficiently controlled, the yield of phenol and acetone will decrease.

To avoid the danger of explosion due to the great activity of sulphur dioxide, the reaction had to be restrained. This was achieved by dropping cumene hydroperoxide into an atmosphere of sulphur dioxide gas. Preference was given to a method in which the liquid flowed in a film over a cooled surface and the catalyst could be absorbed by the liquid.

The assembly is shown in Fig. 7.

Sulphur dioxide gas, dried by passing it through a wash bottle with concentrated sulphuric acid, was run via a capillary flow meter into a vertical glass tube with an inside diameter of 2 cm. At the top of the tube cumene hydroperoxide was

added dropwise from a dropping funnel, so that the liquid flowed down the wall in a thin layer. The outside of the tube wall was cooled by means of water, kept at 10°C. The reaction mixture was collected in a flask placed in ice under the tube.
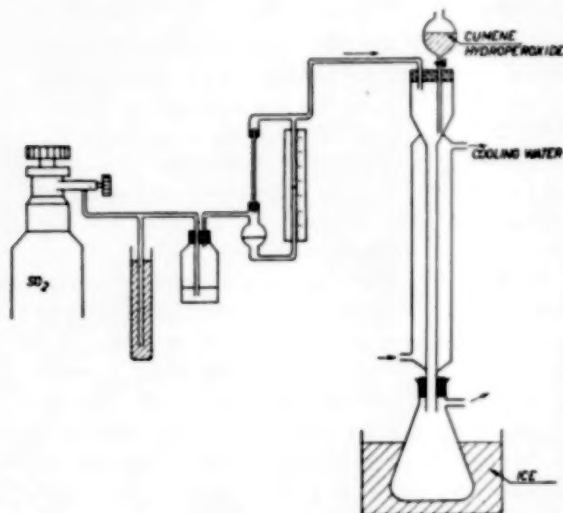

Fig. 7. Decomposition of cumene hydroperoxide by means of sulphur dioxide

In this apparatus 25 g cumene hydroperoxide was passed through in 73 minutes. The tube was filled with sulphur dioxide gas which was supplied during the reaction at the rate of $1\frac{1}{2}$ litres per hour.

The reaction mixture from the flask was fractionally distilled, the sulphur dioxide being expelled during the first stage of heating. The mixture was then separated into the following fractions :

    I. 6·0 g boiling below 60°C.
   II. 1·43 g boiling range 60-170°C, mainly water
  III. 11·81 g boiling range 170-185°C.
  IV. 5·65 g residue.

The first fraction consisted almost entirely of acetone (63 per cent of the theoretical quantity); the third mainly of phenol (70 per cent of the theoretical quantity). The residue was a black resinous material.

Quantitative determinations of the reaction

mixtures of experiments carried out by the above method gave the results collected in Table 5.

Table 5
Decomposition of cumene hydroperoxide by sulphur dioxide.

Cumene hydroperoxide added in g	Time of addition in min.	Yield of acetone %	Yield of phenol %
20·0	53	56·4	67·8
20·0	120	57·8	82·5
20·75	110	67·2	82·6

Sulphur dioxide was passed through at the rate of $1\frac{1}{2}$ litres/hour. After expulsion of absorbed SO_2 the iodide reaction on unconverted hydroperoxide in the mixture gave a negative result. The mixture was then neutralized by means of n-caustic potash to the litmus end point and the acetone distilled off till a temperature of 95°C had been reached. The acetone was collected in a measuring flask which was made up to 1 litre after the distillation. The acetone content in the aqueous liquid was determined by the hydroxylamine method [19]. The distillation residue was placed in another measuring flask and the phenol content in the liquid determined by bromatometric titration [20].

The yields of phenol and acetone in the experiments with pure cumene hydroperoxide point out that undesired side reactions take place. Further mitigation of the reaction can be obtained either by diluting the sulphur dioxide with an inert gas, or by dissolving the cumene hydroperoxide in an organic solvent.

Since cumene hydroperoxide is always obtained as a solution in an excess of cumene, it would be favourable from a technical point of view if the oxidized cumene could, without further operations, directly be decomposed into phenol and acetone. We have therefore carried out a number of experiments in which pure cumene hydroperoxide was dissolved in cumene in various concentrations and the liquids were decomposed as described above by means of sulphur dioxide.

The SO_2 was again passed through at the rate of $1\frac{1}{2}$ litres/hour. The temperature of the cooling water for the film reactor was 10°C.

At the end of the experiments the bulk of the absorbed sulphur dioxide was removed by gentle heating. The reaction mixture was then neutralized with dilute alkali. On further heating the acetone distilled over; this acetone was determined by the hydroxylamine method mentioned before.

The residue was made alkaline by adding a fresh quantity of dilute alkali so as to be sure that all the phenol had dissolved in the aqueous layer.

The cumene was now pipetted off; the remaining aqueous layer placed in a measuring flask and made up to 1 litre with distilled water. The phenol in this liquid was determined bromatometrically as in the previous series of experiments.

A survey of the results of the decomposition of cumene hydroperoxide solutions in cumene by SO$_2$ is given in Table 6.

Table 6

Decomposition of cumene hydroperoxide solutions by SO$_2$.

Concentration of cumene hydroperoxide in the solution % wt	Quantity solution added in g	Time of addition in min.	Yield of acetone in %	Yield of phenol in %
28·7	34·96	80	84·4	93·3
40·1	29·95	50	71·0	83·7
42·2	26·80	90	68·5	90·6
50·0	23·98	22	66·6	81·0

These figures show clearly that the yield is increased by slow addition and lower concentrations of cumene hydroperoxide.

Continuous Procedure for the Preparation of Phenol from Cumene

In order to be able to study the overall process an apparatus was developed for the continuous preparation of phenol and acetone from cumene on a small scale. The procedure was based on the results of the experiments discussed in the foregoing chapters.

Experimental

The apparatus consisted of three sections:
1. an oxidation section
2. a film reactor for the decomposition of cumene hydroperoxide
3. a section for the processing of the decomposition products.

Purified cumene was used as base material for all the experiments.

Re 1. The oxidation section—For the oxidation reaction we used at first a copper reaction vessel of about 400 ml capacity provided with a copper stirrer. The cumene and the oxidizing gas could be fed continuously at the bottom of the reactor, while provisions had been made for circulation of the oxidized liquid.

Batch experiments of only one or two hours yielded very satisfactory results. In long-time or continuous experiments, however, the packing of the stirrer and of the circulating pump caused much trouble. The rate of oxidation decreased rapidly as a result of contamination of the cumene by attacked packing material.

Another apparatus was therefore designed which had no moving parts, so that during the oxidation the cumene was in contact only with copper.

The reactor consisted of a vertical copper tube 1,250 mm long and with an inside diameter of 24 mm. The tube was sealed at both ends by means of flanges; copper rings were used as packing material. By an electrically heated jacket the tube could be heated to the desired temperature. Cumene and the oxidizing gas were fed at the bottom of the reactor, while the oxidized liquid and the excess of gas were discharged at the top. Before each test the inside of the copper tube was etched with fuming nitric acid.

Oxidation experiments have been carried out in this reactor with oxygen and with air as the oxidizing gases; in some cases the surface area was enlarged by filling the tube with copper turnings. The results were satisfactory in all cases; operating continuously no decrease in oxidation rate was observed during a run of 11$\frac{3}{4}$ hours.

The apparatus is very simple. This type of reactor presents possibilities for application on a larger scale.

189

Re 2.   The film reactor—In the oxidation section cumene containing 20-30 per cent wt cumene hydroperoxide is produced continuously. The function of the film reactor is to decompose the dissolved cumene hydroperoxide into phenol and acetone. For this purpose we have designed an apparatus which can be imagined to consist of two parts :

1. a device for the supply of the liquid to be decomposed and for spreading it to form a film ;
2. the reactor proper, which consists of a vertical tube surrounded by a water jacket.

The film was produced by letting the oxidized liquid flow along the outer wall of a cone. In this way a thin liquid layer was formed, which could then flow along the inside of the reactor as a connected film.

Sulphur dioxide was introduced at some distance from where the liquid film was formed, so that decomposition could not take place until the hydroperoxide had reached the cooled zone.

In this reactor experiments were carried out with solutions of cumene hydroperoxide of various concentrations and at different through-puts of the liquid and of the catalytic gas.

The capacity of the film reactor proved to depend on the hydroperoxide concentration in the liquid to be decomposed, on the temperature of the cooling water and on the throughput of the SO_2.

Re 3.   The section for the processing of the decomposition products—In the first experiments a simple distillation at atmospheric pressure was applied for the processing of the decomposition products. In a column 190 cm long, packed with Raschig rings, the acetone was first distilled from the reaction mixture. From the remaining liquid the cumene was distilled off in another column. On continuous distillation of the residue we finally obtained a fraction which contained mainly phenol. Moreover, a large quantity of tar was formed.

It had been shown (Table 6) that the decomposition of cumene hydroperoxide under the influence of sulphur dioxide could give a very good yield of phenol.   Since now the yield of phenol was considerably lower, it was concluded that con-densation reactions had taken place during the processing.   From the material balances it was also evident that part of the cumene had been condensed to higher boiling products.

It was actually possible to separate from the tarry residue a fraction with the properties of a dimer of cumene or α-methyl styrene (mol wt 233 ; % H 8·5, % C 90·9 ; n_D^{20} 1·5660 : after hydrogenation : mol wt 252, n_D^{20} 1·5095).

Such condensation products are naturally undesirable, since they have an adverse influence on the yield of the entire process [21].

A considerable improvement in the yields was obtained by distilling the reaction mixture originating from the film reactor at a pressure of 20 mm.

A further improvement was observed when the decomposed solution was first treated with anhydrous soda till CO_2 was no longer formed. The solution was then filtered and finally distilled at a pressure of 20 mm.

Treatment with anhydrous soda seems more favourable than washing with a dilute soda solution, because in the latter case the acetone and part of the phenol dissolve in the aqueous solution which will make the separation of these products more difficult.

Moreover, after the soda treatment a reaction mixture is obtained from which pure products no longer smelling of SO_2 can directly be recovered.

HEAT EFFECTS

For the technical preparation of phenol from cumene the heat effects of the various reactions are of importance. By applying HESS's law, these heat effects can be determined from the heats of combustion of the reacting substances.
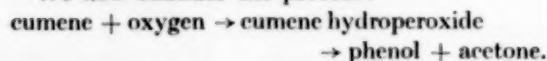
According to literature data the heats of combustion are :

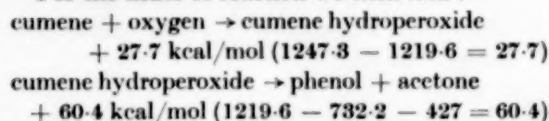|		
cumene	1247·3 kcal/mol	
phenol	732·2 ,,	[22]
acetone	427 ,,	

For the heat of combustion of pure cumene hydroperoxide an average value of 1219·6 kcal/-mol* was found.

---

* The heat of combustion of cumene hydroperoxide was measured by *Koninklijke/Shell-Laboratorium, Amsterdam*, according to ASTM D 240/50.

We now consider the process :

cumene + oxygen → cumene hydroperoxide
→ phenol + acetone.

For the heats of reaction we then find :

cumene + oxygen → cumene hydroperoxide
+ 27·7 kcal/mol (1247·3 − 1219·6 = 27·7)

cumene hydroperoxide → phenol + acetone
+ 60·4 kcal/mol (1219·6 − 732·2 − 427 = 60·4)

These values are relatively inaccurate, for they have been determined as the small differences

The thermal effect of the decomposition reaction is more than twice as great as that of the oxidation reaction.

Technical Procedure

The technical realization of the " cumene process" for the preparation of phenol and acetone naturally requires more extensive laboratory experiments and particularly pilot plant work than has been described.
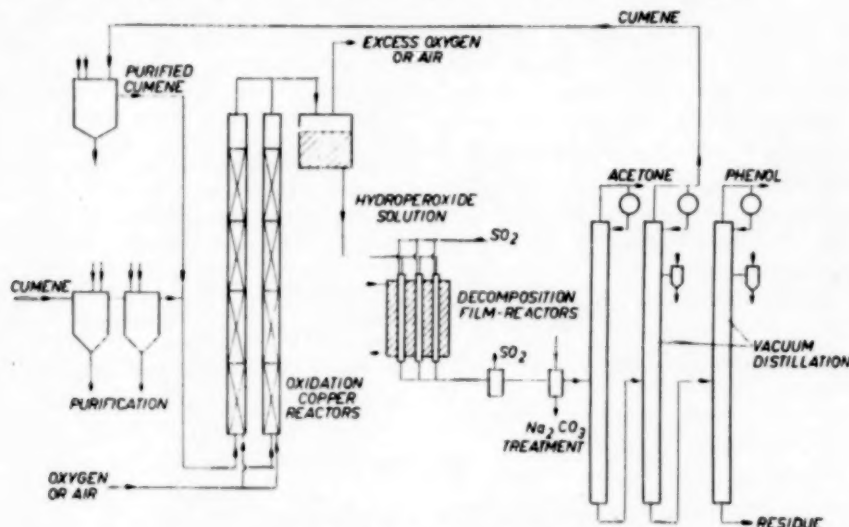

Fig. 8.   Flow sheet of the cumene process.

between two or three large numbers. The errors in the heats of combustion accumulate in the values of the heats of reaction calculated by this method. Moreover, we have based our calculations on the assumption that the conversions take place quantitatively.

When we leave these inaccuracies out of consideration, however, the following rough data for the design of technical equipment are available :

1. During the oxidation of cumene to cumene hydroperoxide 27·7 kcal is liberated per g mol cumene hydroperoxide formed ;   this is 182 kcal per kg cumene hydroperoxide formed.

2. During the decomposition of cumene hydroperoxide into phenol and acetone 60·4 kcal is liberated per g mol cumene hydroperoxide converted ;   this is 400 kcal per kg cumene hydroperoxide converted.

However, on the basis of the results obtained the following procedure, schematically represented in Fig. 8, can be given [23] :

a. Purification of the base material

The base material cumene, to be suitable for oxidation, should meet certain requirements. The purification method to be adopted depends on the impurities to be removed from the crude cumene.   Air, oxygen, or, if necessary, another oxygen-containing gas mixture can be used as the oxidant.

b. The oxidation

A number of long copper tubes can be used as reactors.   At the bottom pure cumene and the oxidizing gas are fed continuously. The reaction temperature is preferably 120°C.

At the top of the reactor the oxidized cumene is discharged.

c. *The decomposition*

From a buffer vessel the hydroperoxide solution is fed to a number of film reactors in which the decomposition takes place under the influence of SO_2 as a catalyst.

d. *Processing of the reaction products*

After the decomposition the liquid is first slightly heated so as to remove the bulk of the SO_2 absorbed.   This is followed by a treatment with anhydrous soda till the liquid gives a neutral reaction.   After filtration the reaction mixture is rectified.   At a slightly elevated temperature the acetone distils over first ; from the remaining liquid the unconverted cumene is distilled off in a second column in vacuum.   This cumene can be re-used after purification.

In a third column the phenol is separated from the residue.

The authors wish to express their gratitude to

REFERENCES

[1] Chem. Eng. News 1950 **28** 3665; Petroleum Times 1951 **55** 1174.   [2] HOCK, H. and LANG, S.; Ber. 1944 **77 B** 257.   [3] Br.P . 610,293.   [4] Br. P. 630,286.   [5] Br. appl. 32604/48.   [6] Belg. P. 501,871; Germ. appl. A. 2620.   [7] Germ. appl. 5,150/51.   [8] WAGNER, C. D., SMITH, R. H. and PETERS, E. D.; Anal. Chem. 1947 **19** 976.   [9] FRANCIS, A. W.; Chem. Revs. 1948 **42** 126. [10] ARDAGH, E. G. R. and BOWMAN, W. H.; J. Soc. Chem. Ind. 1935 **54** 267 T.   [11] SLEICHER, E.; Ber. 1886 **19** 673.   [12] To be published.   [13] Br. P. 587,584.   [14] KHARASCH, M. S., FONO, A. and NUDENBERG, W.; J. Org. Chem. 1950 **15** 748, 763.   [15] Br. P. 626,095; 629,429.   [16] Br. appl. 32600-01/48.   [17] Belg. P. 507,993.   [18] Belg. P. 497,509.   [19] MARASCO, M.; Ind. Eng. Chem. 1926 **18** 701.   [20] REDMAN L. V., *et al.*; J. Ind. Eng. Chem. 1913 **5** 389.   [21] See also Br. P. 670,444.   [22] Int. Crit. Tables Vol. V, 162 (1929).   [23] See also Chem. Eng. 1951 **58** 11, 215.

CORRECTION

We regret that in Vol. 2, No. 3 page 108, the date of receipt of the paper by Dr. J. Anderson Storrow was wrongly given.   It should read "7 July. 1952."